

Jan Regtmeier¹
Ralf Eichhorn²
Martina Viefhues¹
Lukas Bogunovic¹
Dario Anselmetti¹

¹Experimental Biophysics and Applied Nanoscience, Faculty of Physics, Bielefeld University, Bielefeld, Germany

²Nordita, Stockholm, Sweden

Received January 21, 2011

Revised May 31, 2011

Accepted June 1, 2011

Review

Electrodeless dielectrophoresis for bioanalysis: Theory, devices and applications

Dielectrophoresis is a non-destructive, label-free method to manipulate and separate (bio-) particles and macromolecules. The mechanism is based on the movement of polarizable objects in an inhomogeneous electric field. Here, microfluidic devices are reviewed that generate those inhomogeneous electric fields with insulating posts or constrictions, an approach called electrodeless or insulator-based dielectrophoresis. Possible advantages compared to electrode-based designs are a less complex, monolithic fabrication process with low-cost polymeric substrates and no metal surface deterioration within the area of sample analysis. The electrodeless design has led to novel devices, implementing the functionality directly into the channel geometry and covering many areas of bioanalysis, like manipulation and separation of particles, cells, DNA, and proteins.

Keywords:

Bioanalysis / Dielectrophoresis / Electrodeless / Insulator-based

DOI 10.1002/elps.201100055

1 Introduction

The trend towards miniaturized bioanalytical fluidic devices has increased the interest in dielectrophoresis (DEP) [1–3]. The term, first adopted by Pohl in 1951 [4], refers to the motion of a polarizable object in an inhomogeneous electric field [5, 6]. Pohl was one of the first to apply this long known phenomenon to bioanalytical problems [3], in his case the characterization and separation of cells [5]. This is a typical application of a “Lab-on-a-Chip” or “micro Total Analysis System” [7–12]. The concept is to fabricate miniaturized fluidic devices in a chip format that are capable of handling and analyzing especially biological and clinical samples, integrating steps from sample injection and preparation to separation, detection, and analysis. The benefits are low sample consumption, separation, and detection with high resolution and sensitivity, low costs and short times of analysis [13].

In order to achieve this integration, different sample processing steps have to be combined into a single device. The list of possible steps includes: trapping, immobilization, concentration, focusing, characterization, and separation. Regarding cellular analysis, further processing may be

necessary, like cell lysis or cell fusion. DEP is a powerful technique and allows the realization of all the above-mentioned procedures, with the perspective that different processing steps may be merged into one single continuously operating lab-on-a-chip device [14].

DEP is non-invasive and non-destructive. Typical objects for bioanalysis are colloidal particles (often for proof-of-concept), bacteria, viruses, spores, eukaryotic cells, DNA, RNA, and proteins. In aqueous solution, all of them are polarizable, i.e. a dipole can be induced by an external electric field. This intrinsic particle property implies that no special sample preparation or chemical/biological modifications are necessary (label-free technique) so that particle properties remain unchanged during DEP-manipulation, an important aspect for further processing.

There are two main strategies to generate the inhomogeneous electric fields required for DEP: microelectrodes and insulating topographical structures (see Fig. 1). Microelectrodes have been the standard method because of the established microelectronic fabrication techniques. But in 1989, Masuda et al. introduced the idea of using insulating constrictions for DEP (see Fig. 1A) [15]. They microfabricated a constriction with an opening at the center, applied a voltage and trapped and fused a pair of cells. It took a decade for this idea to spread, but the possibility to implement device functionality into the device layout has given momentum to its development. This approach is nowadays called electrodeless or insulator-based DEP [16–18]. In this context, electrodeless means that there are no metal surfaces at the location of dielectrophoretic

Correspondence: Lukas Bogunovic, Experimental Biophysics and Applied Nanoscience, Faculty of Physics, Bielefeld University, Universitätsstr. 25, 33615 Bielefeld, Germany

E-mail: bogunovic@physik.uni-bielefeld.de

Fax: +49-521-106-2959

Abbreviations: DEP, dielectrophoresis; eDEP, electrodeless dielectrophoresis

Colour Online: See the article online to view Fig. 1 in colour.

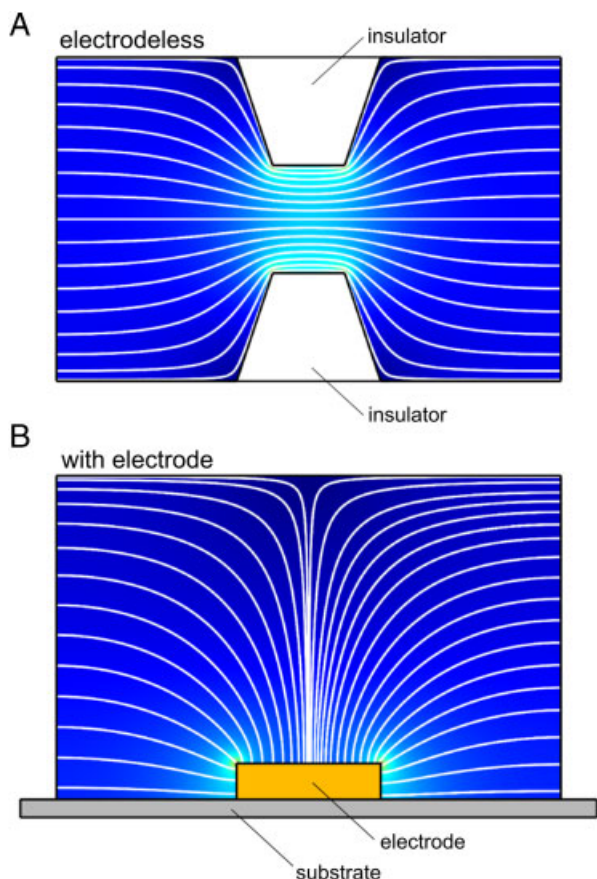


Figure 1. Illustration of the concepts of electrodeless (A) and microelectrode-based (B) dielectrophoresis. The white lines indicate the electric field lines and the color code represents ∇E^2 (increasing from blue to yellow).

manipulation of the sample (although electrodes are obviously needed to apply the electric fields somewhere in the device). In the following, we will use the term electrodeless DEP (eDEP) synonymously for insulator-based DEP.

There are several advantages of eDEP compared to standard (microelectrode based) DEP. (i) The devices are less complex to fabricate because no metal deposition is necessary. Instead the electric fields can be applied by placing metal wires in the outlet reservoirs. (ii) A monolithic fabrication is possible opening up the possibility to mass fabricate the devices by injection molding or hot embossing from low-cost plastics, e.g. PDMS, PMMA, or Zeonor [56]. This is especially important for clinical applications where disposable plastic devices are mandatory. (iii) There is no surface fouling of electrodes due to electrochemical effects especially for buffers with physiological salinity. Therefore, no electrochemical side effects are generated at the location of DEP manipulation (e.g. change in pH or generation of bubbles). (iv) Constant field gradients can be generated over the full height of a microchannel; for microelectrodes, the DEP force decays exponentially with the height above the electrode [1]. (v) eDEP allows the simultaneous electrokinetic (electrophoretic and electroosmotic) actuation of

fluids and particles over large distances by applying DC voltages. For microelectrodes an additional hydrodynamic flow is often necessary for sample handling. A disadvantage of eDEP is, compared to microelectrode-based DEP that relatively large electric potentials are necessary to generate equivalent electric field strengths and the consequent limitation of the frequency range because of the limited slew-rates of high-voltage equipment [19]. However, as reviewed below, there are already devices combining operation in the MHz range with the concept of eDEP [20, 21].

This review focuses on microfluidic devices and applications explicitly exploiting electrodeless dielectrophoresis in the sense of the definition above. Any omission is unintentional and we apologize in advance to the respective authors if we overlooked their deserving work. Readers interested in DEP in general may consult the reviews [1, 2, 3, 22, 23, 129]. Our paper is organized as follows: first the theory of DEP is presented (see Section 2) with a focus on the specifics of eDEP, and we describe how the basic physical forces (DEP, transport, and diffusion) can be balanced to achieve the anticipated application (trapping, focusing, and separation). Then, the available device designs are summarized (see Section 3 and Table 1) and different design considerations are discussed. In Section 4, the published applications are reviewed organized according to the type of sample (particles, cells, DNA, and proteins) followed by Section 5 where a critical bird's eye view of the current developments in eDEP is presented.

2 Theoretical background

The following overview is not intended to give a complete account of the theory of dielectrophoresis for the different particle species (colloids, cells, DNA, proteins, etc.) under the various experimental conditions reported in the literature. We rather discuss those theoretical aspects we consider most important for a physical understanding of the experiments on eDEP reviewed in Sections 3 and 4. This theoretical background is presented from a modeling perspective of the particle motion in eDEP devices under the influence of the most prominent forces, and is summarized by comparing the relevance of these forces for the different applications of eDEP.

The typical experimental situation is the following: eDEP is performed in a topographically structured microfluidic device with length scales of the order of 0.1–100 μm , fabricated of an insulating material. Aiming at biophysical applications, a physiological buffer solution is usually used with homogeneous, isotropic electrical properties of an ideal conductor. Correspondingly, the Debye length of the electric double layer at the walls of the microfluidic device and at the particle's surface is much smaller (typically a few nm) than the length scale of the microstructure and, in most cases, the particle size. Exceptions are DEP experiments with proteins that have a typical size of only a few nanometers

Table 1. Microfluidic chip layouts for electrodeless dielectrophoresis



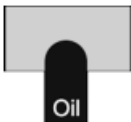
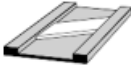

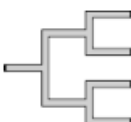
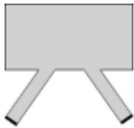
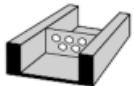

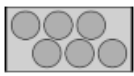
Layout	Icon	Sample	Material	Application	Mode	Reference	Remark
(a) Posts		Particles	Glass	Trapping	Batch	[60]	
		Particles	Glass	Trapping/concentration	Continuous	[17, 18]	
		Particles	Glass	Trapping/concentration	Batch	[79]	
		Particles	Glass	Trapping/concentration	Batch	[61]	
		Particles	PDMS	Separation	Batch	[–] ^{a)}	
		Particles	n/a	Separation/optimization	Continuous	[73]	Simulation
		Particles	Glass	Trapping	Batch	[74]	Selectivity study
		Particles	Glass	Trapping	Batch	[72]	Trapping zones study
		Particles	PDMS	Separation	Batch	[82]	
		Cells	PDMS	Trapping/fusion	Batch	[27]	1 MHz AC
		Cells	PDMS	Focusing	Continuous	[95]	
		Cells	Glass	Separation	Batch	[47, 100, 101, 103]	[100] Concentration
		Cells	Glass	Separation/trapping	Continuous	[102]	
		Particles/cells	Cyclo-olefin	Trapping/concentration	Batch	[94]	
		DNA	Glass	Trapping	Batch	[16]	
		DNA	PDMS	Separation/polarizability	Batch	[31, 32]	
		(b) Blocks/tips		DNA	Glass	Trapping/concentration	Batch
Proteins	Glass			Trapping	Batch	[24]	
Particles	PDMS			Separation	Continuous	[83, 84]	
Particles	PDMS			Separation	Continuous	[85]	
Particles	PDMS			Focusing	Continuous	[81]	
Particles	PDMS			Trapping/separation	Batch	[89]	Series of tips
				Separation	Continuous	[105]	Simulation
Cells	Glass, photoresist			Trapping/fusion	Batch	[15, 97]	2 MHz AC [15]; 450 kHz [97]
Cells	PDMS			Separation	Continuous	[106]	
Cells	SU8			Trapping	Batch	[46]	
Cells	SU8/PDMS			Separation	Batch	[46]	
Cells/DNA	PDMS			Trapping/lysis/extraction	Batch	[103, 112]	
DNA	Glass			Separation	Continuous	[114]	
(c) Oil droplet		DNA	PDMS	Trapping/concentration	Batch	[113]	
		Particles	PDMS/oil	Trapping	Batch	[75]	
		Particles	PDMS/oil	Separation	Continuous	[76]	
(d) 3D barrier		Particles	Cyclo-olefin	Separation	Continuous	[86]	
		Particles/cells	Glass	Trapping/concentration/separation	Continuous	[109]	
		Particles	Glass	Migration analysis	Continuous	[122]	
		DNA/protein complexes	PDMS	Separation	Continuous	[115]	
(e) Serpentine/sawtooth/circular		Particles	PDMS	Separation	Continuous	[92]	
		Particles	PDMS	Focusing/separation	Continuous	[91]	
		Particles	PDMS	Separation/migration	Continuous	[93]	
		Particles	PDMS	Separation	Continuous	[90]	
				Separation	Continuous	[87]	Simulation
				Separation	Batch	[88]	Simulation
(f) Hierarchical network		Cells	PDMS	Focusing	Continuous	[110]	
		Particles	PDMS	Concentration	Continuous	[80]	

Table 1. Continued

Layout	Icon	Sample	Material	Application	Mode	Reference	Remark
(g) Liquid electrodes		Particles	SU8/PDMS	Focusing	Continuous	[20]	2 MHz AC
		Cells	SU8/PDMS	Separation	Continuous	[21]	2 MHz AC
		Cells	PDMS	Separation	Batch	[48]	Contactless DEP
		Cells	PDMS	Trapping	Batch	[28]	Contactless DEP
(h) Membrane		Cells	SU8	Trapping/concentration	Batch	[78]	
(i) Nanopipette		DNA	Glass	Trapping	Batch	[77]	
		Proteins	Glass	Trapping	Batch	[25, 26]	
(j) Particle constrictions		Cells	Glass/PET	Selective trapping	Batch	[98]	
		Cells	Glass/PET	Selective trapping	Batch	[99]	

a) L. Bogunovic et al., paper submitted.

[24–26]. An electric voltage is applied via electrodes that are placed outside the structured region in the device where the dielectrophoretic manipulation of the sample actually takes place. This voltage consists of a superposition of a static and an oscillating component

$$U(t) = U_{DC} + U_{AC} \cos(\omega t) \quad (1)$$

where the frequency $\omega/2\pi$ does not exceed 2 MHz in all the experiments described below. The voltage difference between the electrodes creates an electric field \vec{E} within the device that gives rise to electrokinetic effects, the most prominent being electrophoresis (see Section 2.2), electroosmosis (see Section 2.3), and dielectrophoresis (see Section 2.4). In some of the experiments (e.g. [27, 28]), an additional hydrodynamic driving force is imposed on the particle by an external pressure difference applied to the device (see Section 2.3). All experiments are performed at room temperature, so that thermal noise effects notably influence particle motion as well (see Section 2.5).

In the following, we discuss these different contributions to the total force governing the dynamical behavior of the particle in the device in more detail, focusing on the regime relevant for eDEP with bio-particles as characterized above. In that regime, the following assumptions [29] are well satisfied (and often made tacitly):

- (i) The particle size is small compared to the length scale of non-uniformities of the external electric field \vec{E} .
- (ii) The “external” charges (or currents) that create the field \vec{E} are not affected notably by the particle charge, so that the external field \vec{E} is not altered by the presence of a particle.
- (iii) Transient re-arrangements of the (free and polarization) charges within the device are much faster than time variations of the electric field [30].

- (iv) The electrostatic approximation is valid (see also the following section).

2.1 Electric field

For frequencies in the range of MHz, the corresponding wavelength of the electric field is of the order of 1 m or larger, so that the electrostatic approximation is perfectly valid on the scales of micro- and nano-fluidic devices. The actual time dependence of the electric field $\vec{E} = \vec{E}(\vec{r}, t)$ due to the voltage (1) enters parametrically

$$\vec{E} = \vec{E}_{DC} + \vec{E}_{AC} \cos(\omega t) \quad (2)$$

where

$$\vec{E}_{DC} \propto (U_{DC}/U_*)\vec{E}_* \quad \text{and} \quad \vec{E}_{AC} \propto (U_{AC}/U_*)\vec{E}_* \quad (3)$$

with identical proportionality factor. This proportionality factor depends on that part of the whole microfluidic device for which the “reference” field \vec{E}_* is calculated, and is given by the ratio between the “reference” voltage U_* and the voltage that needs to be applied to the device electrodes in order to create the voltage drop U_* over the device part for the reference field. It can be estimated by mapping the microfluidic layout to an electric circuit diagram where distinct ohmic resistances are assigned to topographically different sections of the fluid channels [31, 32].

The static “reference” field \vec{E}_* is calculated by solving the Laplace equation

$$\Delta\Phi = 0 \quad (4)$$

for the electric potential $\Phi = \Phi(\vec{r})$, and using

$$\vec{E}_* = -\nabla\Phi \quad (5)$$

The reference voltage U_* is fixed by Dirichlet boundary conditions for (4) at “inlet” and “outlet” channels of the

microstructured region, which are connected to the electrodes. In case of a spatially periodic microstructure, one may as well restrict field calculation to a few periods of the structure and impose U_* by Dirichlet boundary conditions for that device part. At the interfaces between buffer solution (electrolyte) and device material Neumann boundary conditions have to be used, i.e. the component of the electric field normal to the material surface vanishes, $\vec{n} \cdot \nabla \Phi = 0$ (\vec{n} denotes the unit vector normal to that surface). This is a consequence of the electrolyte solution being an ideal conductor with uniform electrical properties (conductivity σ) and the material being a perfect insulator, so that the electric current density is given by $\vec{J} = \sigma \vec{E}$ within the electrolyte and $\vec{J} = 0$ within material regions. Again assuming that charge distributions are quasi-stationary at any instance in time (see point (iii) above), charge conservation $\dot{\rho} + \nabla \cdot \vec{J} = 0$ implies $\nabla \cdot \vec{J} = 0$ everywhere, and thus $\vec{J} \cdot \vec{n} = 0$ at the device walls.

This result expresses the fact that the ions carrying the electric current cannot penetrate into the solid material. The electric current, and due to the proportionality between \vec{J} and \vec{E} also the electric field, are thus constraint to those regions in the device that are accessible to the fluid. In view of the additional condition $\nabla \cdot \vec{J} = 0$ or, equivalently, $\nabla \cdot \vec{E} = 0$ it is evident that non-uniform electric fields in the structured region of the device are created by varying fluid-accessible cross-sections due to constrictions, posts, obstacles, branchings, etc. or by curved channels. This principle forms the physical basis for *electrodeless* dielectrophoresis.

2.2 Electrophoresis

For Debye lengths much smaller than the particle size, the electrophoretic velocity \vec{v}_{EP} (with respect to the fluid) is given by the famous Helmholtz–Smoluchowski result [33]

$$\vec{v}_{EP} = \frac{\varepsilon \zeta}{\nu} \vec{E} \quad (6)$$

which is independent of particle size and shape [34]. The proportionality factor $\mu_{EP} = \varepsilon \zeta / \nu$ between particle velocity and electric field \vec{E} is called the electrophoretic mobility; ε is the permittivity of the fluid, ν its kinematic viscosity, and ζ is the ζ -potential [33, 35] of the electric double layer surrounding the particle. Although the electrophoretic motion is induced by an electric field, μ_{EP} is only loosely related to the actual charge of the particle (hidden in the ζ -potential [33]), but essentially depends on properties of the electric double layer around the particle and the electrolyte.

For the time-dependent electric field (2), the electrophoretic motion contains an oscillating back-and-forth component, which does not contribute to a systematic displacement of the particle. It is thus mostly irrelevant on the typical time scales of interest (of the order of seconds), and one usually focuses on the time-averaged electrophoretic velocity

$$\vec{v}_{EP} = \frac{\varepsilon \zeta}{\nu} \vec{E}_{DC} \quad (7)$$

when studying electrokinetic effects in microfluidic devices. Net electrophoretic particle motion is therefore controlled by the DC component of the electric field.

2.3 Electroosmosis and hydrodynamic flows

Due to the low Reynolds numbers in microfluidic devices and negligibly small inertia effects (overdamped motion), the particle practically behaves like a fluid element and instantaneously follows the fluid flow. The particle velocity $\vec{v}_{HD} = v_{HD}(\vec{r})$ resulting from hydrodynamic flows is therefore given by

$$\vec{v}_{HD} = \vec{v}_{EOF} + \vec{v}_{pressure} \quad (8)$$

where the velocity field of the fluid is, in the general case, a superposition of an electroosmotically and a pressure-driven flow, \vec{v}_{EOF} and $\vec{v}_{pressure}$. Under certain conditions, the electroosmotic flow \vec{v}_{EOF} is proportional to the electric field \vec{E} everywhere in the device, resulting in $\vec{v}_{EOF} = -(\varepsilon \zeta / \nu) \vec{E}$, where ζ is the ζ -potential at the device walls [36]. Apart from the assumptions of thin and quasi-steady electric double layers, the most important additional condition for this similitude to hold is a homogeneous interface between device material and buffer solution [36], with the consequence that ζ is uniform within the whole device. In that case, electroosmotic effects can be absorbed into the electrophoretic velocity, and both linear electrokinetic effects together can be described by a velocity relation of the form (7) with ζ being reduced by the ζ -potential ζ at the device walls. As a consequence electrophoresis may be compensated by electroosmosis if ζ and ζ are of comparable size, so that there is no observable net effect from linear electrokinetics.

2.4 Dielectrophoresis

As already mentioned, DEP refers to the motion of polarizable (uncharged) particles in non-uniform electric fields. For a polarizable particle with effective polarizability α , the dielectrophoretic force can be written as [5, 6]

$$\vec{F}_{DEP} = \alpha (\vec{E} \cdot \nabla) \vec{E} \quad (9)$$

expressing the effect of the non-uniformities of the electric field \vec{E} on the effective dipole $\alpha \vec{E}$ induced by \vec{E} . For the low frequencies used in eDEP up to at most a few MHz, the charges (ions) are able to follow the electric field changes virtually instantaneously (see approximation (iii) above) and lossless (also dielectric losses are negligible as they come into play only at higher frequencies [37]). This justifies describing the effective polarizability α in (9) as a real-valued, scalar (isotropic) quantity. In general, α is a function of the frequency ω of the electric field that may even change sign. However, for simple particles with no internal structure, like colloids, and up to not too large frequencies,

this dependence is extremely weak so that α can very well be approximated as being independent of ω . The frequency beyond which this approximation breaks down depends on the conductive and dielectric properties of buffer solution and particle [37], and is typically found around 10–100 kHz under eDEP conditions.

The situation is much more complicated for complex particles like DNA and cells. DNA may be deformed from its unperturbed configuration or even completely stretched, so that the time scale of these deformation processes come into play. Accordingly, frequency dependencies of the DNA polarizability or DEP force have been observed already for small frequencies in the order of several 10 to 100 Hz, as summarized in [121]. Similarly, the inhomogeneities of cells and the associated differences of conductivity and permeability of their internal structures entail a more complicated dependence of effective polarizability α on the frequency of the external field [3].

The dielectrophoretic force (9) is equivalent to a dielectrophoretic energy

$$W_{\text{DEP}} = -\frac{1}{2}\alpha\vec{E}^2 \quad (10)$$

Depending on the sign of α , the particle is thus attracted to regions with high electric field strengths ($\alpha > 0$, positive DEP) or low electric field strengths ($\alpha < 0$, negative DEP). The fact that the square of the electric field enters in (10) indicates that dielectrophoretic effects can be observed for both, DC and AC fields. Indeed, time-averaging the square of the electric field from (2) yields

$$W_{\text{DEP}} = -\frac{1}{2}\alpha(\vec{E}_{\text{DC}}^2 + \vec{E}_{\text{AC}}^2/2) \quad (11)$$

where we used the approximation mentioned above that α is independent of ω . (For general time-dependent electric fields, the time-averaged expression is obtained from (10) by replacing \vec{E} with the rms electric field.)

This result covers two (limiting) cases which both are frequently used in eDEP experiments: purely DC induced DEP

$$W_{\text{DEP}} = -\frac{1}{2}\alpha\vec{E}_{\text{DC}}^2 \quad \text{for } U_{\text{AC}} = 0 \text{ (or } U_{\text{AC}} \ll U_{\text{DC}}) \quad (12)$$

and DEP dominated by the AC field

$$W_{\text{DEP}} = -\frac{1}{2}\alpha\vec{E}_{\text{AC}}^2/2 \quad \text{for } U_{\text{DC}} \ll U_{\text{AC}} \quad (13)$$

see also (3). The typical situation in the latter case is that the applied DC voltages U_{DC} are of the order of 10 V, whereas AC voltages U_{AC} of several hundreds of volts are used.

In the same sense as the electrophoretic mobility (see Section 2.2) also the effective polarizability α is not a pure particle property but is influenced by the electric double layer and the surrounding buffer solution. It is, for instance, known to depend on the concentration of ions in the solution, its pH value and viscosity [16], and may even contain contributions due to fluid motion within the

electric double layer [38]. The study of various system characteristics with respect to their relevance for the effective polarizability is an active field of research. To mention just a few recent examples, aspects of particle ζ -potential, Debye length, and electrolyte composition are investigated in [39], the influence of electroosmotic flows at the particle surface in [40–42], and the frequency dependence of dynamic double layer effects in [43]. The impact of particle inhomogeneities and disturbing device boundaries is summarized in [3].

For estimating (the order of magnitude of) α it is often sufficient to refer to the simplest possible situation, disregarding all these (more detailed) aspects, and, in particular, the presence of the electric double layer. For instance, a spherical (colloidal) particle in the electrolyte solution may be approximated by a conductive dielectric sphere in a conductive dielectric medium. The effective dipole moment $\alpha\vec{E}$ can then be identified as that moment that generates the same dipole field around the particle as a point-dipole [29]. For the low frequencies of eDEP, polarization effects are dominated by conductive processes [3]. In the intermediate frequency regime both, conductive and dielectric processes, contribute and give rise to a complex frequency dependence of α [3], and the effective polarizability of a conductive dielectric sphere with radius a in a conductive dielectric medium is given by [3, 29, 44]

$$\alpha = -2\pi\epsilon a^3 \frac{\sigma_p - \sigma}{\sigma_p + 2\sigma} \quad (14)$$

where ϵ and σ are the permittivity and conductivity of the fluid, respectively, and σ_p is the conductivity of the particle. The latter vanishes for insulating particles (like colloidal beads made of latex, polystyrene, SU-8, etc.), so that (14) reduces to

$$\alpha = -2\pi\epsilon a^3 \quad (15)$$

In Table 2, we use this formula to estimate the polarizability of colloidal particles. (For high frequencies, dielectric effects dominate such that the polarizability is governed by the permittivities ϵ and ϵ_p of fluid and particle, respectively, $\alpha = 4\pi a^3(\epsilon_p - \epsilon)/(\epsilon_p + 2\epsilon)$.)

2.5 Diffusion

In view of the thermal energy at room temperature being $kT = 4\mu\text{m fN} = 4\text{nm pN}$ (k is Boltzmann's constant), it is obvious that thermal fluctuations play a non-negligible role in micro- (and nano-) fluidic environments. They induce diffusive (Brownian) motion of the particle, which may even lead to thermal noise-driven escapes out of potential minima of the energy landscape, the particle is subjected to [45], e.g. the dielectrophoretic potential (11). The thermal fluctuations for a particle with diffusion coefficient D and friction coefficient η are usually modeled by a force term $\eta\sqrt{2D}\vec{\xi}(t)$ [45], where $\vec{\xi}(t) = (\xi_x(t), \xi_y(t), \xi_z(t))$ are three mutually independent

Gaussian white noises with zero average $\langle \xi_i(t) \rangle = 0$ and correlation $\langle \xi_i(s) \xi_j(t) \rangle = \delta_{ij} \delta(t-s)$ ($\langle \cdot \rangle$ denotes ensemble averages over many realizations of the noise and $i, j \in \{x, y, z\}$).

Complementary to these fluctuating noise forces, there is energy dissipation into the thermal heat bath. It is quantified by a friction force $-\eta \dot{\vec{r}}$ [45] proportional to the momentary particle velocity with respect to the fluid, $\dot{\vec{r}}$. Both effects are connected by the Einstein relation

$$D = \frac{kT}{\eta} \quad (16)$$

between the diffusion coefficient D and the friction coefficient η [35, 45]. In general, the Stokes result $\eta = 6\pi\nu a$ gives a reasonable approximation for the friction coefficient of a particle (radius a) suspended in a fluid (viscosity ν). For a specific experimental setup, η can be determined more precisely from measuring the diffusion coefficient D and using the relation (16).

2.6 Force balance

The force contributions experienced by the particle in the microfluidic device as detailed above may be summarized in the following way. A deviation of the momentary particle velocity $\dot{\vec{r}}$ from the total driving velocity $\vec{v}_{EP} + \vec{v}_{HD}$ implies a friction force of $-\eta[\dot{\vec{r}} - (\vec{v}_{EP} + \vec{v}_{HD})]$ which is balanced by the remaining forces acting on the particle, essentially DEP and thermal fluctuations. For the full equations of motions we furthermore have to take into account short-ranged interaction forces \vec{F}_{wall} with the walls of the microdevice, whereas inertial effects are negligibly small (overdamped limit). We therefore find $0 = -\eta[\dot{\vec{r}} - (\vec{v}_{EP} + \vec{v}_{HD})] - \nabla W_{DEP} + \vec{F}_{wall} + \eta\sqrt{2D} \vec{\xi}(t)$. Solving for the highest time-derivative we obtain the Langevin equation

$$\eta \dot{\vec{r}} = -\nabla W_{DEP} + \vec{F}_{wall} + \eta(\vec{v}_{EP} + \vec{v}_{HD}) + \eta\sqrt{2D} \vec{\xi}(t). \quad (17)$$

The corresponding illustrative physical picture is that of a particle diffusing in a potential landscape with barriers and wells, given by the dielectrophoretic energy W_{DEP} (and by the interaction with the walls). The directed transporting forces due to electrophoresis, electroosmosis, and fluid flows effectively correspond to a “tilt” of that potential. In the experiments, the strength of the thermal noise driving diffusion is basically set by room temperature, whereas the electrokinetic forces are controlled by the experimentalist via the external voltage (1) and hydrodynamic flows by external pressure differences. Depending on the application one is aiming at, the relative strengths of the dielectrophoretic energy landscape, the “tilting forces” (electrophoresis, electroosmosis, hydrodynamic flows) and the thermal fluctuations have to be carefully balanced to create distinct experimental conditions:

Trapping: In order to “permanently” immobilize particles the dielectrophoretic potential wells have to be deep

Table 2. Polarizabilities of different species

Species	Polarizability [10^{-31} Fm^2]	References
Microparticle (1 μm)	−5560	Calculated for polystyrene ^{a)}
Nanoparticle (10 nm)	−0.0056	Calculated for polystyrene ^{a)}
Cell (10 μm)	5 560 000	[3, 108]
DNA long (5–164 kbp)	6–30 000	[31, 32] (and References therein)
DNA short (<5 kbp)	0.1–2	[49] (and References therein), [124, 125]
Proteins ^{b)}	0.0001–0.07	[24, 25, 123]

These are only rough estimates as the polarizabilities strongly depend on buffer conditions (ionic strength, viscosity, multi-valent ions), DNA conformation, cell viability, cell type and frequency of the electric field.

a) homogeneous dielectric particle in a conductive medium, see Eq. (15).

b) Eq. (18): kT for room temperature and electric field strengths E_{trap}^2 estimated from the protein trapping experiments in Refs. [24, 25, 123].

enough to overcome all the other forces. Accordingly, the “tilting forces” are typically switched off (i.e. $U_{DC} = 0$, no external pressure difference). Thermally driven escapes out of the potential wells should only occur very rarely and on very long time scales, a condition that at least requires

$$|\alpha| E_{\text{trap}}^2 \gtrsim kT \quad (18)$$

where E_{trap} denotes the field strength corresponding to the depth of the dielectrophoretic trap.

Focusing: In order to focus the particles into concentrated, confined streams, diffusive spreading has to be suppressed. DEP is combined with directed transporting forces to drive the particles into and through narrow potential “valleys” that are oriented along the direction of the transporting force.

Skulan et al. quantitatively compare theoretical simulations in 2D and experimental results of fields in a faceted microchannel [122]. They determine the electric field induced velocity of 200 nm latex beads with particle image velocimetry (PIV). By solving the Laplace equation they simulate the electric field of the experimental geometry. The simulations are in good agreement to the experimental data of PIV, within variations based on fabrication process, but fail for pressure-driven flow.

Separation: For the separation of a mixture of different particle species, the applied force combination has to be selective for the property the particle species differ in. Note that in view of (8), particles of different sizes have identical velocity in a hydrodynamic flow. Similarly, electrophoresis in a homogeneous buffer solution cannot distinguish between particles of different shape or size but with identical ζ -potential (see (6)), as it is the case for the important particle class of DNA molecules [33]. On the other hand,

dielectrophoretic forces are expected to show a quite prominent dependence on particle size (cf. (14) and (15)), which is the motivation to exploit them for particle sorting purposes. To have a notable effect on the particle motion, their strength should at least be of the order of the transporting forces. However, if dielectrophoretic effects are too strong, we are in the trapping regime and separation is impossible, since all particles become immobilized. This means that DEP and, e.g. electrophoresis (being the most important realization of a transporting driving in this context) have to be precisely balanced to achieve a selective average particle velocity or migration path through the tilted potential landscape. It is convenient to exploit the pure AC regime of DEP (see (13)), because then electrophoretic and dielectrophoretic forces can be controlled independently by adjusting U_{DC} and U_{AC} respectively (cf. (3)).

3 Devices

3.1 Design considerations

When designing an eDEP device, there are several important points to address:

- (i) polarizability of the sample (particles, cells, DNA, proteins, etc.),
- (ii) strength and geometry of the electric field necessary to achieve the desired application (trapping, focusing, separation),
- (iii) continuous-flow or batch operation of the device,
- (iv) substrate and reusability of the device,
- (v) buffer and coating,
- (vi) Joule heating.

In the following, we address these items in detail.

Polarizability: As very rough estimates, the polarizabilities for different sample objects are summarized in Table 2 covering 10 orders of magnitude. It is important to note that those polarizabilities sensitively depend on the ionic strength of the buffer (especially divalent ions), frequency of the applied field, particle size and exact species or conformation (e.g. of DNA fragments [32]). Regarding cells, the situation is even more complex. Their polarizabilities additionally depend on membrane conductivity and permittivity, cytoplasm conductivity, and consequently on the cell species and state [5, 6] (e.g. different cell types or dead and live cells of the same type have different polarizabilities [46–48]). Note that polarizability data are often measured with techniques and setups quite different from typical eDEP conditions. For instance, DNA polarizabilities are usually obtained using ensemble methods like transient electric birefringence [49–51], conductivity dispersion [52], impedance measurements [53], and time domain reflectometry [54]. Only in few cases, eDEP trapping experiments have been used to estimate DNA polarizabilities [31, 32] observing single molecules.

Electric field: The anticipated applications require to match the strength of the DEP effects relative to transport forces and diffusion (see Section 2.6). If the relevant particle characteristics (polarizability, electrophoretic mobility, etc.) are known, the electric field (strength) suitable for the desired manipulations can be estimated. On the other hand, the electric field in the microfluidic device resulting from a specific device design and from the voltage amplitudes applied to the device can be calculated by the procedure described in Section 2.1. However, it is (to our experience) difficult to predict the precise correspondence between voltage amplitudes and electric field strength or dielectrophoretic forces. Only an order of magnitude estimate can be achieved. As a main reason we point out that a double layer of charges accumulates at the metal electrodes, accompanied by an unknown voltage drop. Furthermore, although the process of microstructuring can be controlled very well, the exact shape of obstacles, constrictions etc., depends on all the fabrication details, especially at sharp corners of the structure, where the impact on the electric field (strength) and the resulting DEP force is most prominent.

Batch or continuous-flow processing: Concerning the processing of the sample in the device, there are two different strategies. In the so-called batch processing, a small amount of sample is injected and analyzed before the next sample volume is injected. In contrast, continuous-flow operation refers to the situation where the sample is processed while continuously flowing through the device. Since particle trapping is obviously run in batch processing mode, while focusing needs continuous-flow conditions, this design aspect is most relevant for particle separation by eDEP. Although both modes can be used for particle sorting, continuous-flow separation offers a few advantages [14]. For instance, complex samples can be separated into different outlets so that further processing steps on the separated species can easily be integrated, which is highly relevant especially for industrial applications. Moreover, the experimental parameters can be tuned and optimized in real time, until the desired separation task is achieved.

Substrate/disposable or reusable devices: The microfabrication of the devices is mainly limited by the availability of the processing techniques and facilities. Glass and silicon were traditionally used for microfluidic chips taking over established methods from microelectronics. These devices are mechanically robust, chemically inert, and reusable, but they are also expensive. Plastics are often the least expensive substrate material, combining the advantages of mass production (e.g. injection molding or hot embossing) and disposability. The latter is especially important for clinical applications because it minimizes issues of sterilization and clogging [55]. Poly (dimethylsiloxane) (PDMS) is the most common plastic for eDEP devices, although there are alternatives (e.g. SU8 or cyclo-olefin (trade name Zeonor)) [56, 94]. For more information about microfabrication, we refer to the general reviews [55–57] and the one from Simmons et al. for polymeric DEP devices [127].

Buffer/coating: It is important to note that all materials have different ζ -potential [58, 59] and therefore different electroosmotic flow properties (see Section 2.2). Consequently, the operation parameters have to be adapted and optimized for the specific material and buffer conditions. Lapizco-Encinas et al. thoroughly study the effects of pH, conductivity of the medium and the applied electric field strength on the electrophoretic and electroosmotic mobility and on eDEP trapping. They study the pH values between 6 and 9, conductivities in the range of 25–100 $\mu\text{S}/\text{cm}$ and field strengths of 200–850 V/cm . Lower pH values turn out to be beneficial for DEP trapping because of the reduced EOF and they concluded that the ideal operating conditions in the presence of EOF are to employ the maximum conductivity and the lowest pH value possible (see also Joule heating) [60, 61]. Mela et al. characterize the ζ -potential and the induced electroosmotic flow in a cyclo-olefin device. Lower voltages were needed to trap particles by eDEP compared to a glass device under comparable conditions because electroosmotic flow effects are reduced [62].

The unspecific adsorption of the sample depends on the substrate and buffer conditions as well as sample properties, and is critical for reversible trapping experiments with proteins (M. Viehaues et al., paper submitted) [63]. Coatings as well as physical surface modifications (e.g. oxygen plasma) can effectively hinder the adsorption (please consult the reviews [64–67] for details). For example, the impact of the dynamic surface coating (Pluronic F127) on cyclo-olefin regarding eDEP trapping is studied by Davalos et al. [68]. They demonstrate that the application of dilute amounts of the triblock copolymer significantly reduced the electric field necessary for particle trapping.

Joule heating: Applying an electric field to a microfluidic system inevitably leads to Joule heating (resistive heating) and consequently to an inhomogeneous temperature distribution. The latter leads to temperature-dependent variations in conductivity of the medium, the ζ -potential, the viscosity, the liquid permittivity and Brownian motion (for the scaling of the properties we refer to [19]). The inhomogeneous variations of those properties disturb the electric field as well as – if applicable – the flow fields. Consequently, the force balance of DEP, electrophoresis, and electroosmosis is disturbed locally.

The dissipated energy (per unit volume) causing Joule heating depends quadratically on the applied electric field [19]. Since the dielectrophoretic energy scales with \vec{E}^2 as well, regions of high dielectrophoretic energy coincide with regions of localized Joule heating making control of Joule heating an important aspect concerning the optimization of eDEP applications.

The minimization of Joule heating is a rather complex problem and there are different routes to pursue. Joule's first law states that the dissipated energy scales linearly with the ohmic resistance and quadratically with the current. The current can be minimized by using low conductive media. Consequently, some eDEP applications demonstrated use low conductive solutions, often even DI water. For many

biological applications, however, highly conductive media are necessary for example for living cells or to assure the functionality of proteins [24]. Therefore, a compromise has to be found regarding the biological aspects and the minimization of heating.

A second possibility is to reduce the applied electric field necessary for the anticipated application, e.g. trapping. Davalos et al. demonstrated that a Pluronic F127 coating reduces EOF in a Zeonor 1060R device [68]. Because reducing EOF changes the force balance of DEP, electrophoresis, and electroosmosis (see Section 2), the coating reduced the electric field necessary to trap particles by eDEP. Thus, the vast literature on the control of EOF can be useful to minimize EOF in terms of the optimization of Joule heating. Because the polarizability as well as the EOF depends sensitively on the ionic strength and pH of the liquid (via charge displacement in the electrical double layer), Sabounchi et al. studied these aspects with the fluorescent dye rhodamine B as an optical thermometer in an eDEP device [69]. They demonstrated good agreement between FEM simulation and experiment and confirmed that Joule heating generates an inhomogeneous temperature distribution. Hawkins and Kirby theoretically studied the effects of Joule heating in a eDEP device by coupling fluid, heat, and electromagnetic phenomena via temperature-dependent physical parameters [19]. Their results indicate that the temperature distribution strongly depends on fluid conductivity and the magnitude of the electric field. They also study explicitly the electrothermal flow, i.e. fluid flow induced by temperature gradients, and could theoretically reproduce vortices often observed in DEP applications, whenever high electric fields are applied.

Interestingly, according to Hawkins and Kirby, the electrothermal flow effects enhance negative DEP particle deflection and trapping in most cases using a constriction in channel depth for eDEP [19]. There are further examples, where Joule heating is not considered as a nuisance but can beneficially be exploited, for example to use it as a heat source for PCR or to catalyze chemical reactions [70].

Concerning device design, heat transfer is another approach to control Joule heating. Already in 2003, Erickson et al. published a study comparing the heat transfer in PDMS/PDMS chips and PDMS/glass devices [71]. The vast majority of heat rejection is through the lower substrate of the chip, which is significantly hindered using PDMS because of the low thermal conductivity. They propose simple guidelines for improving and optimizing chip design concerning heat management.

3.2 Device designs

As explained in Section 2.1, any kind of insulating obstacle in a microfluidic channel leads to an inhomogeneous electric field. This freedom has led to a wide variety of devices. An overview, including the materials and the applications of the devices, is given in Table 1. A first

group of devices (see Table 1(a)) exploits regular arrays of posts. Various post shapes have been introduced (circle, square, triangular) (see Figs. 2, 3 and 4) in order to control the electric field gradient near the posts. Interesting effects can arise, when the array of posts is (slightly) tilted relative to the main channel axis [18]. Orifices in the microfluidic channel due to blocks and tips are another approach (see Table 1(b), Fig. 5). The same idea, but with an adjustable block size, was realized with oil droplets (see Table 1(c), Fig. 6). 3D hurdles and ridges (see Table 1(d), Fig. 7) usually require more sophisticated microfabrication facilities, but open up another degree of freedom in the sample processing.

Besides obstacles in a channel, the channel shape itself can be used to generate DEP forces. Examples are circular or serpentine channels (see Table 1(e), Fig. 8) or hierarchical channel networks (see Table 1(f)). These designs are also suitable for continuous processing. An interesting variant of eDEP is the so-called liquid electrode approach, where the metal microelectrodes of usual DEP are replaced by equipotential surfaces in the fluid. These “liquid electrodes” can be created at apertures of suitable designed side channels in the device (see Table 1(g)), which are connected to the external voltage source via metal electrodes.

An insulating porous membrane generates electric gradient forces with a high number of parallelized DEP regions (see Table 1(h)). Nanopipettes (see Table 1(i)) possess extremely small apertures and are ideally suited to manipulate objects with low polarizability, for example proteins [25, 26]. The self assembly of colloidal particles allows the generation of extended areas of DEP manipulation sites without any need for sophisticated microstructuring (see Table 1(j)).

An interesting aspect of all those different approaches to eDEP is that the functionality of the device is implemented in the device design, i.e. essentially its geometry. Commercially and non-commercially available simulation and modeling tools allow an a priori optimization before the actual experimental implementation [19, 72, 73, 74]. Although the advantages and disadvantages of the different designs strongly depend on the exact realization of the layout and on the envisioned application, some general characteristics of the different designs may be highlighted.

The “classical” eDEP designs (posts, blocks, tips, curved channels) are simplest to fabricate, e.g. via injection molding or hot embossing. Generally, sharp corners in those designs lead to strong electric field gradients and therefore

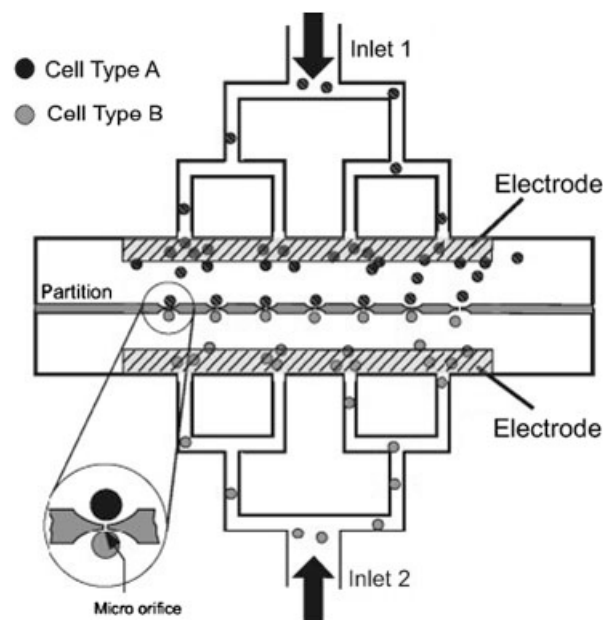


Figure 2. Schematic of a microfluidic device with two hierarchical channel networks to guide pairs of single cells to an array of micro-orifices, where they are trapped by dielectrophoresis. Using a voltage pulse, cell fusion can be initiated. Redrawn with permission from Ref. [27], copyright 2010 American Institute of Physics.

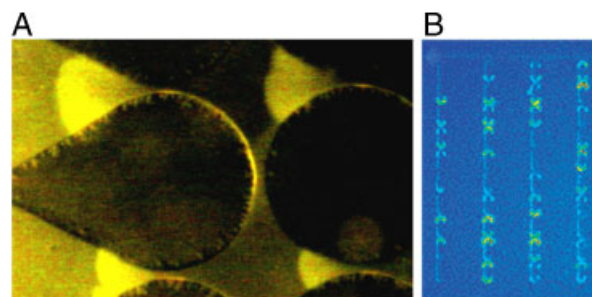


Figure 3. (A) Dielectrophoretic trapping of fluorescently labeled proteins (BSA) in a post array (post diameter $400\ \mu\text{m}$; flow direction from left to right, $E = 700\ \text{V/cm}$). Redrawn with permission from Ref. [24], copyright 2008 Elsevier. (B) Dielectrophoretic trapping of fluorescently labeled DNA (164 kbp) between neighboring rectangular posts (post length $7.4\ \mu\text{m}$; distance between posts $2.3\ \mu\text{m}$; $E = 660\ \text{V/cm}$). Redrawn with permission from Ref. [31], copyright 2006 American Chemical Society.

Table 3. Reviewed eDEP studies ordered according to application and sample species

	Trapping/concentration	Focusing	Separation
Colloidal particles	[17, 18, 60, 61, 72, 74, 75, 79, 80, 89, 109]	[17, 18, 20, 81, 91]	[20, 21, 73, 76, 82–93, 105] (L. Bogunovic et al., paper submitted)
Cells	[15, 27, 28, 46, 78, 94, 97–99, 102, 109, 112]	[95, 110]	[21, 28, 46–48, 100–103, 107, 109]
DNA	[16, 31, 32, 77, 104, 111–114]		[31, 32, 115, 116]
Proteins	[24–26]		

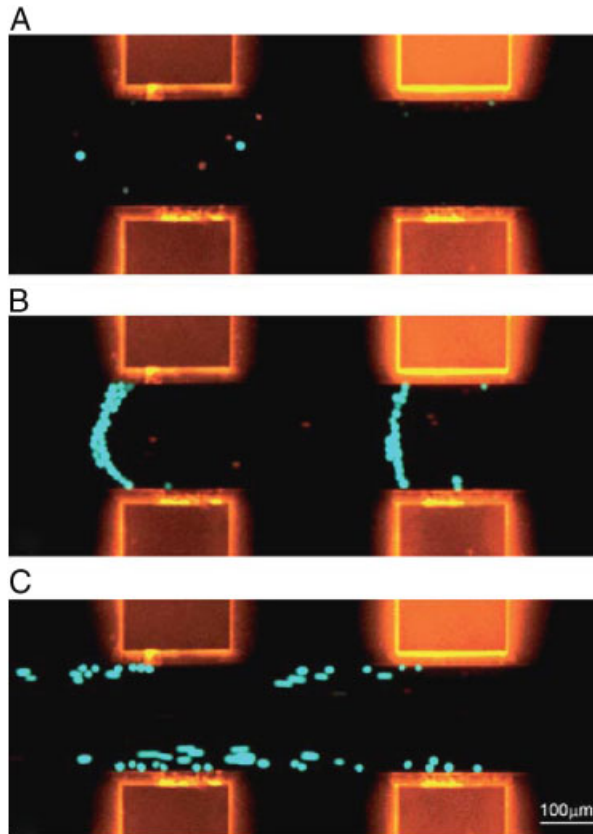


Figure 4. (A) Dead (red) and live (blue/green) THP-1 cells moving from right to left due to pressure driven flow without applying an electric field. (B) 30 s after applying the electric field. The live (blue/green) cells are trapped due to positive DEP, the dead (red) cells pass by the trapping area. (C) Releasing the trapped live cells by turning off the power supply. Redrawn with permission from ref. [48], copyright 2010 Royal Society of Chemistry.

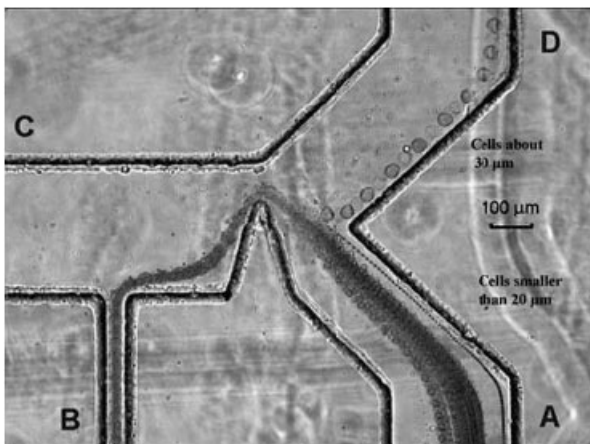


Figure 5. Continuous separation of small and large live breast cancer cells at triangular tip with divergent output branches ($V_A = 56$ V, $V_B = 154$ V, $V_C = 180$ V, $V_D = 0$ V). Redrawn with permission from Ref. [106], copyright 2008 Springer Verlag.

strong DEP forces. The sharpness is, however, most often limited by the achievable precision during the fabrication process. In order to increase the throughput, a parallelization of these designs seems easily possible, for example by microfabricating an array of parallel channels.

The only device design that allows control and adjustment of the “microstructure” during the running experiment is the oil droplet. By changing its volume the constriction size is changed as well [75, 76]. The system, however, lacks the fundamental advantages of most eDEP devices, namely the simple and cost-efficient production. Interestingly, the elastomeric properties of PDMS have not yet been exploited to change size or shape of insulating DEP constrictions.

If high frequencies of the electric field in the MHz range are needed, metallic microelectrodes are better suited than eDEP designs. However, then the advantage of a simple production is lost, and undesired side effects occur, like metal surface fouling or the direct contact of the sample with the metal surface. The latter may be avoided by the liquid electrode designs [20, 21] or capacitive coupling [28, 48].

Concerning very high field strength, the nanopipette is most suitable [25, 26, 77]. However, the problem of fabrication and integration of the pipette into the fluidic device has to be solved, and a parallelization in order to increase the throughput seems difficult. For high parallelization, membranes are an interesting alternative [78] because of the high density of DEP traps. The fabrication and integration, however, is again more difficult.

4 Applications

4.1 Principles

Table 3 gives a quick overview over the applications and samples manipulated and analyzed by eDEP. We categorized the applications into three classes: trapping/concentration, focusing, and separation (see also Section 2.6). These three are qualitatively different tasks. Trapping and concentration imply the holding of the sample at a certain position. Focusing is based on confinement of the sample into a continuous-flow stream. Separation requires selectivity with respect to a specific particle property, such as size, shape, charge, and polarizability. In this sense, a selective trapping mechanism implies separation.

From a physical point of view, this categorization relies on the balancing of different forces including (but not necessarily being limited to) hydrodynamic flow effects, electroosmosis, electrophoresis, DEP as well as diffusion. These forces have different characteristics setting the way they can be exploited and combined, as well as the sample properties they address (as discussed in detail in Section 2):

- (i) size (diffusion, friction, hydrodynamic flow),
- (ii) ζ -potential (electrophoresis, and electroosmosis in case of their similitude [36]),
- (iii) polarizability α (DEP).

4.2 Literature review of applications

In the following, the applications are reviewed categorized according to the manipulated sample. Since colloidal particles often serve as model objects, we begin with those. We then discuss cellular objects where the term 'cell' is understood in a very general sense referring to eukaryotic cells and bacteria, spores and viruses. Finally, applications regarding DNA and proteins are reviewed. Interestingly, we found no applications of eDEP to non-biological samples except the colloidal particles (see Section 4.2.1), as for example carbon nanotubes, synthetic polymers, or assemblies of particles.

The applications of eDEP cover all areas of sample handling and analysis: focusing, concentration, immobilization, trapping, cell fusion, cell lysis, and separation. These can be grouped into non-selective (trapping and focusing) and selective applications (selective trapping and separation). For each sample species, the reviewed research articles are sorted by *trapping/focusing* and *separation*. We use these two categories, and within the categories the order of the device layouts in Table 1, to roughly sort the articles reviewed in the following.

4.2.1 Colloidal particles

4.2.1.1 Focusing and trapping

Cummings et al. are the first to demonstrate streaming dielectrophoresis, i.e. the concentration of particles (200 nm carboxylated latex beads in 1 mM phosphate buffer) into streams by applying a DC voltage to an array of insulating posts [17, 18]. They observe that a tilting of the array with respect to the applied electric field can enhance or deplete particle concentration, and that the efficiency of focusing depends on the shape of the posts. Their theoretical predictions, obtained from solving the Laplace equation for the electric potential, are in good agreement with the experimental observations.

Using AC voltages with very low frequencies between 0.2 and 1.25 Hz of sinusoidal, half-sinusoidal, and saw-tooth signal form (ratchet-type driving), Baylon-Cardiel et al. demonstrate the concentration and immobilization of microparticles in an array of circular posts [79]. They observe different responses according to the signal form. For a sinusoidal signal, the 1 μm -diameter microspheres in distilled water, 2.45 $\mu\text{S}/\text{cm}$, move only back and forth, whereas for half-sinusoidal and saw-tooth signal the microbeads are transported through the device. This experimental behavior is in agreement with the theoretical predictions.

Thwar et al. report particle trapping using two pairs of insulating oil droplets in a configuration similar to a quadrupole [75]. The size and position of the droplets within the PDMS device can be dynamically adapted during the experiment to control the electric field strength and the DEP force. Thwar et al. calculate DEP forces of 15–20 pN for 10 μm polystyrene beads. They also show that a single pair

of droplets is sufficient for continuous particle focusing [76]. However, if additional chemistry is required to be included in the device, e.g. detergents for cell lysis, the stability of the oil droplets may be influenced.

Another focusing technique is presented by Demierre et al. [20]. Instead of using insulating posts or constrictions, they guide the electric field (generated at distant planar metal electrodes) through access channels to the main channel, where the particles are deflected and focused. The equipotential surfaces at the apertures of the access channels serve as "liquid" electrodes. The reduced size of this design allows the generation of eDEP effects at frequencies of 2 MHz, therefore combining the advantages of micro-electrode-based DEP (high frequencies) and eDEP. All experiments are performed in diluted phosphate-buffered saline, 1.4 mS/cm. The results are in very good agreement with the theoretical simulations. An extension of the device design allows the continuous separation of particles from yeast cells [21].

Chen et al. use a hierarchical (tree like) channel network for the continuous concentration of particles by DC eDEP [80]. The particles, 930 nm polystyrene beads in PBS buffer, 1–10 mS/m, flow into an array of parallel channels that merge pair wise into a single channel. Streaming and trapping are observed simultaneously in different regions, as the electric field increases with every merging of a channel pair. The system exhibits a very high trapping efficiency of 100% at 400 V, which is an important aspect in pre-concentration prior to subsequent analytical processes.

Zhu et al. theoretically and experimentally investigate particle focusing at a single microchannel constriction [81]. They study DC as well as AC-based dielectrophoresis. By using AC voltages, the electric field can be chosen much smaller than for DC-driven dielectrophoresis so that Joule heating is reduced.

4.2.1.2 Separation

The separation of microparticles into opposite directions is demonstrated by Bogunovic et al. in a microfluidic ratchet (L. Bogunovic et al., paper submitted) [82]. An array of insulating triangular posts is used to create eDEP traps. A mixture of three different particle species is sorted with the extra twist that any one of them can be forced to migrate oppositely to the other two species by applying a time-dependent AC and DC voltage protocol. All the three separation possibilities are explicitly demonstrated and are compared to theoretical predictions, showing excellent agreement.

Kang et al. continuously separate microparticles by applying DC fields to an orifice formed by an insulating block [83]. The particles, 15.7 and 5.7 μm carboxylated polystyrene beads in 1 mM sodium carbonate buffer, demonstrate negative DEP at the corners of the block and are deflected into distinct reservoirs depending on their size. Simultaneous control of electrokinetic particle transport and DEP-induced

deflection is realized by applying a DC electric field. The particle trajectories are simulated with Lagrangian tracking methods and fit very well to the experimental data. Lewpiriyawong et al. extend the design to three of those orifices in series with the goal to enhance the DEP force and increase controllability [84]. They also demonstrate that a combination of AC and DC voltages can be exploited to reduce the voltage amplitudes required for particle separation, so that joule heating effects decrease. This result is supported by theoretical modeling of the system. In a recent publication, Srivastava et al. report the theoretical and experimental results of separating microparticles at an insulating block [85]. By varying the buffer conductivities, changes in the polarization process are induced for two different electric fields, resulting in buffer-dependent particle trajectories and collection of particles in different outlets. This work points out the possibility of multiparticle separation and multioutlet devices.

Barbulovic-Nad et al. report the first realization of a tunable orifice by using an insulating oil droplet (see Fig. 6) [76]. The device is made via soft lithography with PDMS and the oil is supplied through a Teflon tubing by a syringe. By changing its volume, the electric field and consequently the DEP force can be changed dynamically from 80 to 240 V/cm. With this technique, the authors continuously separate a mixture of two microparticle species using DC voltages. Since this technique is successful even at low electric fields and very flexible it may be a promising tool in bioanalytical applications, e.g. for separating cells sensitive to high electric fields or automated deflection of certain detected particles.

Another degree of freedom concerning device design is used by Hawkins et al. [86]. They implement a 3D hurdle with the shape of a quarter of a circle generating a 100 μm slit over the full channel width (see Fig. 7). The chip is made of Zeonor thermoplastic cycloolefin copolymer. Along the bowed barrier, the angle between DEP force and electrokinetic force varies with the position, which is exploited for continuously sorting microparticles. A separation of 2 and 3 μm beads is theoretically simulated and experimentally shown. The authors state a separation of more than two sorts of particles should be possible.

A different approach for creating inhomogeneous electric fields is to use an unstructured but curved microchannel (see Fig. 8). Due to the electric field gradient generated by the curved channel structure, different particles are focused to different regions of the channel cross section. This effect is exploited for particle separation. Using numerical simulations, Zhang et al. predict the continuous separation of particles in a circular channel [87]. The efficiency strongly depends on the injection point into the circular section but might be increased by operating several circular sections serially. Chen et al. study the concentration and separation of particles in a saw-tooth channel theoretically [88]. Staton et al. experimentally separate polystyrene beads in a similar saw-tooth channel [89]. Their device is made of PDMS with a minimum gap width of 27 μm . Separation is demonstrated for 20 nm, 200 nm, and 1 μm polystyrene beads at 150 V/cm. Zhu et al. study continuous particle focusing in a

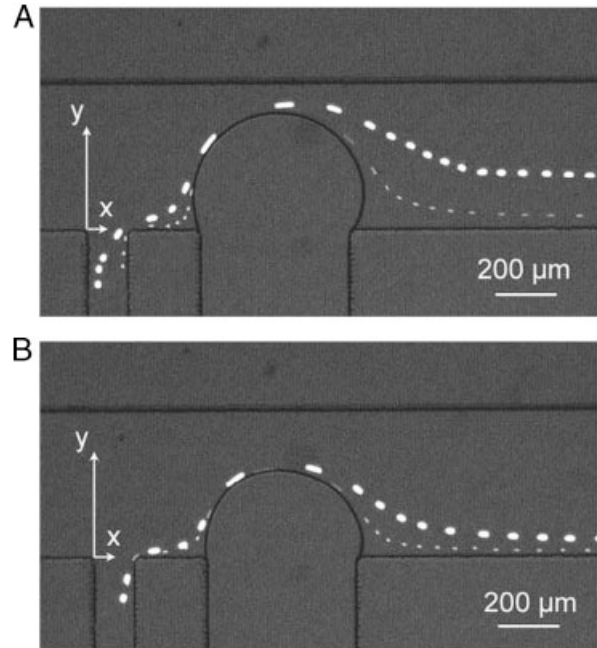


Figure 6. Oil droplet as an insulating constriction used for continuous particle separation by eDEP. Effect of the gap width of (A) 95 μm and (B) 197 μm on the separation of 5.7 and 15.7 μm particles. Redrawn with permission from Ref. [76], copyright 2006 Royal Society of Chemistry.

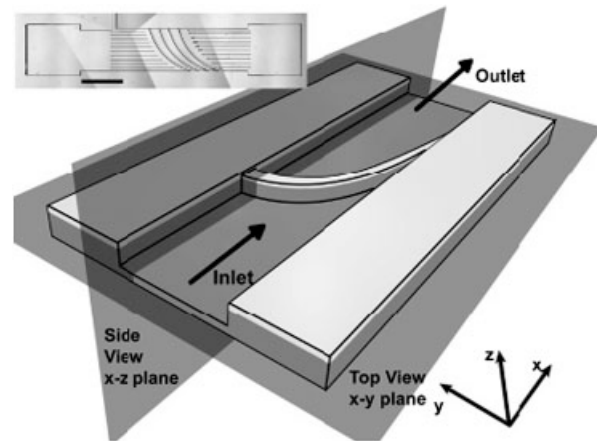


Figure 7. 3D schematic of channel geometry with a bowed constriction generating a slit of 100 μm over the full width of the microchannel. Continuous output streams of colloidal particles are generated with a transverse outlet position specified by electrophoretic and dielectrophoretic particle properties. Redrawn with permission from Ref. [86], copyright 2007 American Chemical Society.

double-spiral channel [90] experimentally and theoretically, and find quantitative agreement. In a follow-up work they demonstrate focusing and separation of 5 and 10 μm as well as 3 and 5 μm polystyrene beads in a double-spiral channel [91]. The particles are first focused via dielectrophoresis to one side of the channel and after passing the first spiral the

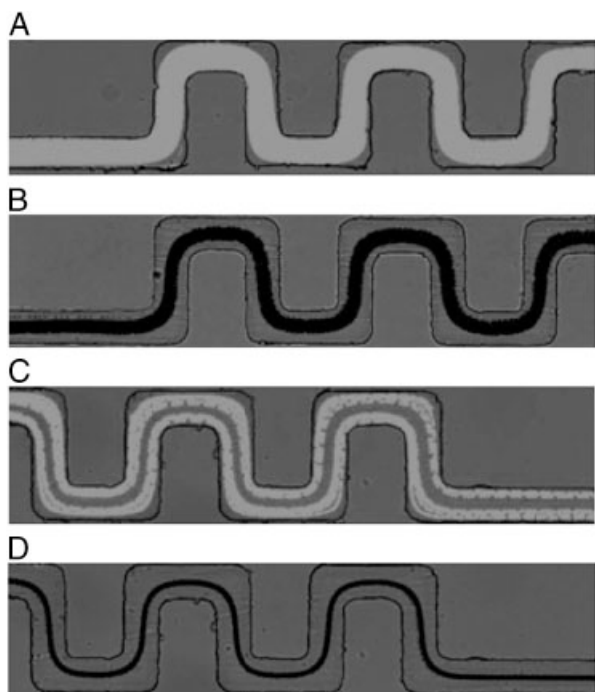


Figure 8. Continuous separation of microparticles in a serpentine channel. (A, B) 2.2 μm (fluorescent) and 5 μm (non-fluorescent) particles at the entrance and (C, D) at the exit of the serpentine channel, respectively. Redrawn with permission from Ref. [92], copyright 2010 IOP Publishing.

particles are separated. In case a pre-concentration step before separation is required this method is thus very efficient. Church et al. use a serpentine channel for continuous particle sorting [92]. Ai et al. numerically calculate particle trajectories in an L-shaped channel by integrating the Maxwell stress tensor over the particle surface [93]. Characteristic trajectories are determined theoretically as well as experimentally for different sized particles.

4.2.2 Cells

4.2.2.1 Focusing and trapping

Sabounchi et al. demonstrate the concentration and selective trapping of *Bacillus subtilis* spores and microparticles in an array of insulating posts (pH 8, conductivity 1–2 $\mu\text{S}/\text{cm}$) [94]. The authors combine eDEP with pressure-driven flow and integrate impedance detection after the pre-concentration, a label-free analysis technique which is rather rare in this context. The advantage of the impedance detection is that it makes fluorescent labeling obsolete, so that the system can easily be integrated into a point of care device without optical components.

Jen et al. realize a similar principle with an array of insulating posts arranged like a series of quadrupoles [95, 96]. They combine hydrodynamic flow and the positive/negative DEP response of dead/living human carcinoma (HeLa) cells in AC electric fields to selectively trap the dead

cells while the living cells are focused and can migrate further through the structure (solution of 8.62% sucrose, conductivity 1.76 $\mu\text{S}/\text{m}$). Nevertheless, the system requires structuring of electrodes parallel to the channel axis “behind” the channel walls, to arrange the AC field perpendicular to the channel.

Probably the first report of eDEP is the work by Masuda et al. from 1989 [15]. They apply an AC voltage with 2 MHz to a small opening at the center of an insulating barrier to trap two cells that form a pearl chain pair. A voltage pulse triggers the fusion of the cell pair, because cell membrane breakdown occurs at the cell-to-cell contact, which is located at the center of the opening. Lee et al. use an identical device for cell fusion and a similar design for cell selection [97]. The applied AC voltages have a frequency of 450 kHz. A parallelized array of those cell fusion traps has been reported just recently (see Fig. 2) [27] where the hydrodynamic flow used to transport the cells to the fusion regions is induced by tilting the whole device. These cell fusion devices enable researches to automatically generate fused cells.

Shafiee et al. demonstrate the selective trapping of three cell species (human leukemia monocytes, breast and breast cancer cells) in a contactless DEP device [28] with additional hydrodynamic transport. Here, the microelectrodes are capacitively coupled to a fluidic channel with a 100 $\mu\text{S}/\text{cm}$ buffer through dielectric barriers, combining the advantages of eDEP with traditional microelectrode-based DEP (high frequencies of the AC voltages). Surface fouling effects and bubble generation are suppressed as well, but electrodes have to be structured during fabrication and additional channels are necessary.

A completely different idea is explored by the group of Masanori Hara [98, 99]. They fill a straight microchannel with glass beads with a diameter of 200 μm . After a quantification of Joule heating for different conductivities between 0.2 and 3 mS/m, their device is used to selectively trap viable yeast cells in a mixture with dead cells. The application of beads to generate field constrictions could be advantageous, e.g. when self-organization of the beads is exploited, eventually even on the nano scale.

Cho et al. demonstrate the concentration of *E. Coli* using an SU-8 membrane with honeycomb-type pores to generate inhomogeneous electric fields (conductivity of medium 0.5 mS/m) [78]. Possible advantages of the membrane are a high parallelization of DEP manipulation sites and strong field gradients for DEP trapping.

4.2.2.2 Separation

The concentration and separation of living bacteria is demonstrated in an array of circular posts [100]. Gram negative as well as Gram positive bacteria show negative DEP under DC conditions, but different minimal DC voltages are required for trapping *E. coli*, *B. subtilis*, *B. cereus*, and *B. megaterium*. This is exploited for their separation. In the same device, trapping, concentration, and separation are shown for *E. coli* and the yeast *S. cerevisiae*

[101], as well as the concentration and separation of live and dead bacteria (*E. coli*) [47] and microalgae [102]. Differences in the DEP response of *B. subtilis* spores and vegetative cells are exploited for their selective trapping [103], and may open the way for efficient separation; likewise for *B. subtilis* and Tobacco Mosaic Viruses [103]. The isolation of live and dead cells is also demonstrated by contactless DEP [48] (Fig. 4). In this study, two post shapes are compared (squares and circles) with the result that the circles yield a higher trapping efficiency. As the conductivities of the cell medium are orders of magnitude higher than those of the cell membranes ($10^3 \mu\text{S}/\text{mm}$ versus $10^{-4} \mu\text{S}/\text{mm}$), DEP devices can distinguish between live and dead cells based on the fact that dead membranes are usually ruptured [100] and therefore show more positive DEP. This class of devices might be a promising tool for the sensitive analysis of samples concerning contamination with e.g. pathogens [103], for which (selective) pre-concentration is an important step in order to enhance sensitivity of the actual analysis.

Chou et al. design two tips, which reduce the channel width to a small aperture in the middle of the channel. They demonstrate trapping and concentration of *E. coli*, and separation of *E. coli* from blood cells [104]. The same device is also used for electrolysing blood cells and for trapping single stranded 1 kbp and double stranded 103 kbp DNA fragments. Jen et al. use an array of those tips for the selective trapping of live and dead HeLa cells in a working buffer of $1.76 \mu\text{S}/\text{m}$ with an AC field of $3.5 \times 10^4 \text{V}/\text{m}$ [46]. The advantage of their design is the open-top that allows further treatment of the cells after analysis. Nevertheless, a structuring of electrodes is necessary. For a theoretical analysis of the DEP forces in such a converging and diverging microchannel we refer to [105].

In contrast to the previously presented work on batch processing techniques, Kang et al. study the continuous separation of cells by specific deflection of the cells via DC eDEP at a rectangular as well as a triangular block, which reduce the width of the microfluidic channel (see Fig. 5) [106]. For fixed (and therefore more stable) white blood cells from an HIV positive patient, the rectangular block separates cells above $10 \mu\text{m}$ from those below $10 \mu\text{m}$ in diameter into two distinct reservoirs. With an optimized triangular block, the continuous separation of live cancer cells below $20 \mu\text{m}$ and above $30 \mu\text{m}$ is achieved. The authors point out that DC dielectrophoresis has limitations concerning the handling of cells, as the large electric fields and joule heating induce stress to the cell membrane. Furthermore, electrolysis at the electrodes may produce radicals that destroy the membrane as well. As a result live breast cancer cells have been observed to die in the constriction generated by the rectangular block (more details on the issue of cells in electric fields can be found in [107, 108]). To reduce cell damage induced by DC fields, the authors propose the application of trehalose instead of sucrose in the working buffer.

Using 3D “hurdles”, Barrett et al. continuously separate *B. subtilis* from 200 nm polystyrene particles (glass device,

pH 7.7, $10 \mu\text{S}/\text{mm}$ conductivity) [109]. The hurdles create a slit of $5 \mu\text{m}$ in height selectively deflecting the different objects. The concept using a shallow hurdle is very versatile and is also suitable for continuous concentration and trapping. Further possibilities arise when the hurdle is tilted by a certain angle. A further advantage is that the height of the slit can be quite precisely adjusted during the etching process.

Church et al. demonstrate the continuous focusing of yeast cells in a serpentine channel [110]. After having been exposed to a $100 \text{V}/\text{cm}$ DC-biased AC electric field during the experiment, 95% percent of the cells were still alive. The same device can be used to selectively focus yeast cells, while *E. coli* cells are not affected and can be filtered out this way. However, the authors do not demonstrate that the selective focusing is switchable so that *E. coli* is focused and the yeasts are not.

4.2.3 DNA

4.2.3.1 Trapping and concentration

The first systematic study on DNA trapping in eDEP devices is conducted by Chou et al. They thoroughly study the dielectrophoretic response of DNA to an AC field up to $1 \text{kV}/\text{cm}$ by trapping single- and double-stranded DNA in an array of insulating posts [16]. They analyze fragments of different lengths, study frequency and viscosity dependence, estimate the trapping force and propose a simple intuitive picture for the polarization process of DNA.

The concentration of DNA by DC eDEP is demonstrated by Gallo-Villanueva et al. in an array of circular posts with even higher field strengths of $2000 \text{V}/\text{cm}$, conductivities of $120 \mu\text{S}/\text{cm}$ and pH in the order of 11 [111]. A negative dielectrophoretic response of the DNA is reported (opposed to the usually reported positive DEP). According to the gel electrophoresis conducted by this group after the DEP treatment, the DNA is not damaged during trapping.

Some groups have integrated eDEP into their cell handling chips for genome manipulation and analysis. For example, Prinz et al. demonstrate the extraction and isolation of chromosome from *E. Coli* by eDEP in an array of tips [112]. They lyse bacteria on the chip by an osmotic shock and trap their DNA in the array to separate it from lysate fragments for further manipulation. Also using an array of tips, Swami et al. enhance the DNA hybridization kinetics and sensor sensitivity through pre-concentration by eDEP trapping [113]. They address the DNA pre-concentration in high-ionic strength buffers and are able to achieve a 10-fold enhancement of DNA hybridization. This demonstrates once more that precise pre-concentration of highly diluted analyte solutions is a key issue for highly sensitive sensor technology and effective (bio-) chemical reactions.

Ying et al. trap very short DNA fragments with a nanopipette [77]. They demonstrate inter alia the trapping of single- and double-stranded 40mer DNA and a

single-nucleotide triphosphate. In particular, the frequency dependence is discussed in detail. The unique advantage of the nanopipette is the extremely strong field gradient that can be created with moderate voltages to trap even small molecules with low polarizability.

All the DNA experiments above suggest once again that DNA polarizability is in general a very complex process that cannot be completely explained using the Clausius–Mosotti factor. Instead further theoretical and experimental investigations remain necessary.

4.2.3.2 Separation

Exploiting that the DNA polarizability depends on the length of the DNA fragments, Regtmeier et al. separate linear as well as supercoiled DNA in an array of insulating posts (see Fig. 3B) [31] with typical separation times in the order of only 200 s. With their simple, sensitive, and versatile device, this group further demonstrates that DNA fragments of equal length but with different spatial conformations (supercoiled versus linear) can be distinguished in the eDEP post array as well [32]. Furthermore, DNA polarizabilities can be estimated from DEP trapping times [31, 32].

Size-dependent trajectories of DNA fragments are observed by Parikesit et al. [114] in their continuously working device. They use an insulating block to generate DEP with very low field strengths in the order of 10 V/cm. Physical mechanisms of confined DNA DEP are addressed by the authors because their channel is only 400 nm high. Interestingly this group finds negative DEP (in contrast to findings reported by other groups), and observes that DNA polarizability increases with decreasing fragment length.

Using a 3D structured PDMS microfluidic device similar to the “hurdle” structures mentioned above, Everwand et al. demonstrate continuous-flow separation of DNA and DNA/protein complexes [115]. The separation is performed at a bowed constriction that reduces the channel height down to 670 nm. Exploiting the change in polarizability induced by proteins bound to DNA, Everwand et al. can distinguish between pure DNA and DNA/protein complexes with eDEP as label-free technique. These results suggest that eDEP may be a very promising technique for investigating DNA interaction properties as an alternative to electrophoretic mobility shift assays (EMSA).

4.2.4 Proteins

Referring to Table 2, the polarizability of proteins is minute, making their DEP manipulation challenging. Nevertheless, there are a few publications utilizing eDEP for trapping proteins.

Lapizco-Encinas et al. manipulate bovine serum albumin (BSA) by negative DC eDEP in an array of circular posts (see Fig. 3A) [24]. They applied electric fields from 700 to 1600 V/cm and determined a dependence of trapping

efficiency and electric field strength. The successful trapping of proteins is due to the remarkably high field strength of 1600 V/cm (for eDEP devices). Lapizco-Encinas et al. systematically vary the conductivity (from 25 to 100 $\mu\text{S}/\text{cm}$), and pH of the buffer (between 8.0 and 9.0). Manipulation of proteins can be optimized for higher buffer conductivity and lower pH-values but also Joule heating effects have to be considered.

Clark et al. report the trapping of proteins (protein G, immunoglobulin G and yellow fluorescent protein) by a nanopipette [25, 26]. It has an aperture with a diameter of 100–150 nm, much smaller in scale than typical eDEP structures in microfluidic devices, yielding field strengths of about 10^6 V/m at the pipette tip by applying only 1 V. For stable proteins the buffer contains 10 mM phosphate, 150 mM sodium chloride and 2 mM sodium nitride at pH 7.2. The trapping is reversible and the proteins keep their functionality despite the high field strength.

5 Critical discussion

So far fundamental aspects of device design (Section 3) and applications (Section 4) were presented. Critical aspects on the level of single applications or single design considerations were already discussed accordingly. Here, we attempt to take a critical bird's eye view on the developments of eDEP and bring together the ideas of devices and applications from the point of view of different user groups (industry, academia, medicine). The discussed aspects are subjective, because, depending on the anticipated application, different features might be judged differently.

The major objective of eDEP is to realize a chip-based microfluidic device that integrates functions (so far) ranging from focusing over concentration to separation. DEP in general offers the advantages of being non-invasive and label free. Electrodeless dielectrophoresis offers further advantages: there are no metal surfaces close to the region of DEP manipulation and consequently no surface fouling and no electrochemical side effects occur. Moreover, the devices can be monolithically fabricated and mass production techniques such as injection molding or hot embossing are applicable.

eDEP adds a considerable value and brings us closer to the often mentioned Lab-on-a-Chip (LOC) or μTAS devices that promise small sample volumes, short analysis times, and high cost-efficiency. Many functionalities and processing steps needed for LOC have already been demonstrated by eDEP so that the integration of different functionalities in a single chip can be envisioned, leading towards point of care devices along the idea of “sample in–answer out”.

In Sections 3 and 4, we have shown the wide variety of ideas to fabricate and operate microfluidic eDEP devices, ranging from single orifices, over post arrays to micropipettes, capacitively coupled electrodes and oil droplets. All these ideas have been demonstrated to function on a proof-of-principle level or even beyond. Nevertheless, specific user

groups have different requirements concerning functionality, flexibility, and ease of handling/production. Before a discussion of the different design concepts from this point of view is presented we attempt to summarize the specific needs of some of the most important application areas.

Industry: There is a growing industry branch that supplies and fabricates microfluidic systems. Only if the microfluidic device outperforms the established techniques, customers are willing to purchase the product. Therefore, major aspects are costs, reliability, reproducibility, analysis time, and simple usage. On the other hand, industry also buys microfluidic devices for standard applications as purification, separation, and quality control. Benchmarks are costs, throughput, continuous working principle, and device reliability and simplicity.

Academia: In academia there are also two subgroups, the scientists who develop new devices, and the highly trained end users. The first group exploits the current limit of knowledge regarding physics, chemistry, engineering, and biology on the small scale looking for novel effects, tries to understand systems that could not be studied before because of technical limitations, and engineers novel highly integrated or parallelized devices. The second group looks for novel tools with a maximum of flexibility and control over the processes performed on the chip. On the other hand, throughput, continuous operation and simplicity are often not required. Benchmarks are therefore flexibility and reliability.

Clinical/medical: The typical user is looking for novel techniques that reduce costs for the financially strapped health care system. The devices are used by non-experts so that “sample in–answer out” devices are mandatory. Moreover, for so-called bedside tests, the analysis time needs to be below 2 min and the used devices need to be disposable. Typical benchmarks are therefore costs, reliability of the supply chain, precision and ease of handling.

In case where a microfluidic system allows a novel test or analysis that could not be performed before, the advantage is clear. But most often, there are already conventional techniques available. In order to be able to identify the advantages of the eDEP devices, we first identify and characterize the standard techniques. As they set the benchmark for the novel eDEP devices, we are then able to discuss possible advantages and disadvantages.

Most eDEP devices demonstrated so far allow the manipulation or separation of cells (regarding colloidal particles as model particles for cells or macromolecules), DNA fragments or proteins. For the separation, purification, and quality control of DNA and proteins, electrophoresis or capillary electrophoresis are probably the most often used and best established techniques. The typical separation time is 30 min and above (up to a few days for large DNA fragments) with sample volumes starting at 1 μL (about 100 ng per lane on a slab gel) [116, 117]. Generally, capillary electrophoresis is – from our point of view – not a single molecule technique. For cell sorting, fluorescent or magnetic activated cell sorting (FACS/MACS) can be

identified as the standard. A large number of single cells flow through a capillary and are sorted according to their optical/magnetic properties. Sorting of about 1000 cells per second is possible, but a fluorescent or magnetic label is required [117]. Both standard methods have been optimized over decades and have reached a very high level of maturity.

DEP and especially eDEP do, however, offer some advantages over the two mentioned conventional techniques. Concerning for example the separation of DNA, eDEP-based separation is almost an order of magnitude faster than capillary electrophoresis [31]. Moreover, separation and manipulation can be handled on a single molecule level. The most promising advantage, scientists and companies are only starting to exploit, is the possibility to integrate different functionalities on a single chip. For example, starting with a whole-blood sample, it is in principle possible to separate the cells in the blood from serum, to extract and amplify the DNA and finally to make an assay with a fluorescent read out in order to identify certain DNA fragments that correlate with an infection or disease. Concerning cell sorting, the obvious advantage of DEP is that no additional labeling is necessary and, again, that further handling or analysis of the sorted cells can be integrated into a single chip.

These very general performance specifications can be made more precise when looking at single devices regarding channel characteristics and the tuning of parameters for specific applications. For instance, for biological samples, as proteins or cells, a careful design is necessary for the exact shape of the insulating obstacles to precisely control electric field gradients. Sharp corners or tips generate extremely high electric field gradients. For the manipulation of only weakly polarizable objects as proteins this is an advantage, although the proper folding of the proteins should be checked after manipulation. Regarding the handling and separation of cells, if the gradient is too high, the cells might be lysed or killed and most obviously the protein contents of a living cell will be changed under such stress. This aspect is important for single-cell proteomics and metabolomics.

Continuously operating devices also have specific characteristics that should be considered. Typically, a force is applied at an angle – often perpendicular – to the direction of flow [14]. Consequently, two force components have to be properly arranged. Remarkably, the implementation of continuous-flow devices is rather simple via eDEP. A single insulating block can be easily fabricated and is sufficient for the continuous separation of e.g. cells (see Table 3). The exact shape of the obstacle can be chosen such that the field strength is appropriate for the application. For pre-concentration and trapping, sample adsorption to the surface can be critical. Surface coatings are needed to control adsorption and guarantee reversible trapping.

Whenever regions of high dielectrophoretic energy are created, Joule heating should be considered, especially for cells and proteins. As already discussed in Section 3, most studies use low conductive media to avoid Joule heating. Consequently, cells are stressed or killed and proteins are

denatured. Therefore, the buffer should be carefully chosen regarding ionic strength, pH, and surface coatings. If no appropriate heat management is realized, additional side effects as electrothermal flow can spoil the anticipated application [70].

A current trend in the field is the further miniaturization. For example for the fast manipulation and analysis of DNA and proteins, this might lead to substantial improvements and novel effects that can be exploited. It should, however, be kept in mind that the dimensions of the device are large enough to ensure a detectable spatial resolution and that diffusion on the nano scale is a fast process. Especially if the smallest dimensions of the device are on the length scale of the Debye layer, which can be about 100 nm for DI water, an overlap of the Debye layers of opposing walls should be considered [118, 119].

In order to achieve a real advantage compared to the discussed conventional techniques, the integration of different functionalities on a single chip should be pursued. Especially eDEP might allow the design of lab-on-a-chip devices implementing different functionalities directly in the chip geometry. This offers the advantage that although numerous applications are integrated, the chip can be easily mass-fabricated as e.g. no microelectrodes are necessary.

Regarding the different samples, we noted already that proteins have hardly been addressed. Their analysis might be a valuable next goal (see Table 3). Besides the biological applications, the handling and analysis of non-biological samples as nanotubes or nanowires could be interesting, e.g. for specifically arranging those for molecular circuits and molecular assembly (we could not find any reports in the literature concerning this topic). And although Joule heating might be a nuisance, interesting combinations of trapping and simultaneous heating might allow novel routes in chemical reaction control [70].

For a fast development process from the idea to a working prototype, further efforts on theoretical aspects might be helpful. The polarization mechanisms of DNA and proteins are still controversially discussed [120, 121], although they are the basis for quantitatively exploiting DEP. Another central aspect regarding the quantitative optimization of eDEP devices is to quantify the voltage drop at the electrodes (an unknown fraction of the applied voltage already drops across the electrical double layer) in eDEP applications. Finally, the modeling of the full chip including DEP, electrophoresis, electroosmosis, Joule heating, hydrodynamic flow, and diffusion could help to optimize many aspects of a chip before the first prototype is produced. Many single tools are on the market, but most of them only address certain limited aspects. eDEP is a great example for a very promising technique that involves a vast number of effects that have to be controlled. To us it is still astonishing that such a – principally speaking – simple technique offers the unique possibility to realize almost all operations needed for a fully functional laboratory on a chip.

6 Summary and concluding remarks

We have reviewed microfluidic devices and applications, which exploit the concept of electrodeless dielectrophoresis (eDEP). The term “electrodeless” refers to the defining characteristics that the region of the device in which the DEP manipulation of the sample is performed is free of metallic electrodes. The non-uniformities of the electric field required for DEP are instead created by structuring (with obstacles, constrictions, branchings, etc.) or curving the microfluidic channel (cf. Section 2). The large variety of devices (see Section 3 and Table 1) and applications (see Section 4 and Table 3) reported in the literature impressively reflect this novel freedom in device design compared to standard DEP based on metallic microelectrodes. Many central issues of bioanalysis are covered by eDEP: trapping (immobilization), focusing, and separation is performed with various different sample species, in particular colloidal particles, cellular objects, DNA, and proteins. In designing and operating a DEP device, the (quantitative) understanding of the polarization mechanisms for the different particle species is of great use. Accordingly, this is an active area of research, also from a more fundamental point of view.

An overview of the applications of eDEP published in the literature is given with Table 3. Interesting to note are the gaps in Table 3. For instance, we did not find any report of DNA focusing in the literature, although this task should easily be achievable with current technologies. More interesting are, however, the gaps concerning eDEP manipulation of proteins: there are – to our best knowledge – only three papers on protein trapping/immobilization, and none reporting protein focusing or separation. The reasons are obviously the minute size of proteins and their extremely small polarizabilities (see Table 2), so that large electric field strengths and gradients are necessary for notable DEP manipulation of proteins. Such conditions are actually more easily realizable with metallic microelectrodes than with electrodeless devices, because for the latter topographical structuring on a scale of presumably a few tens or hundreds of nanometers with high precision is necessary. Nevertheless, we think that especially for the manipulation of non-denatured proteins, eDEP can become a valuable tool, as it allows a better control of surface (electro-) chemistry and bio-fouling.

In perspective, the invention of new constriction, obstacle, and channel designs may open up so far unimagined possibilities and may even pave the way towards novel applications. Examples that come to mind are the controlled trapping of single cells (for single-cell analysis), the mixing of different biological components, or DEP-generated “reaction chambers” for biochemical reactions. Another exciting route to follow is the development of more elaborate devices beyond proof-of-principle realizations of single applications that combine and integrate many different processing steps into a “Lab-on-a-Chip” to perform complex bio-analytical tasks. The fact that DEP is label-free and non-destructive, and that it can be

operated in both, batch and continuous-flow mode, renders it a beneficial technique for serial processing steps.

This work was supported by the German Research Foundation (DFG) within the Collaborative Research Center SFB 613 (project D2). For their inspiring collaboration in various eDEP projects, we thank T.T. Duong, H. Höfemann, A. Ros, and P. Reimann.

The authors have declared no conflict of interest.

7 References

- [1] Gascoyne, P., Vykoukal, J., *Electrophoresis* 2002, 23, 1973–1983.
- [2] Lapizco-Encinas, B. H., Rito-Palomares, M., *Electrophoresis* 2007, 28, 4521–4538.
- [3] Pethig, R., *Biomefluidics* 2010, 4, 022811.
- [4] Pohl, H., *J. Appl. Phys.* 1951, 22, 869.
- [5] Pohl, H., *Dielectrophoresis: The Behavior of Neutral Matter in Nonuniform Electric Fields*, Cambridge University Press, Cambridge 1978.
- [6] Jones, T., *Electromechanics of Particles*, Cambridge University Press, Cambridge 1995.
- [7] Reyes, D., Iossifidis, D., Auroux, P., Manz, A., *Anal. Chem.* 2002, 74, 2623–2636.
- [8] Auroux, P., Iossifidis, D., Reyes, D., Manz, A., *Anal. Chem.* 2002, 74, 2637–2652.
- [9] Vilkner, T., Janasek, D., Manz, A., *Anal. Chem.* 2004, 76, 3373–3386.
- [10] Dittrich, P., Tachikawa, K., Manz, A., *Anal. Chem.* 2006, 78, 3887–3908.
- [11] West, J., M. Becker, J., Tombrink, S., Manz, A., *Anal. Chem.* 2008, 80, 4403–4419.
- [12] Arora, A., Simone, G., Salieb-Beugelaar, G. B., Kim, J. T., A. Manz, *Anal. Chem.* 2010, 82, 4830–4847.
- [13] Whitesides, G. M., *Nature* 2006, 442, 368–373.
- [14] Pamme, N., *Lab Chip* 2007, 7, 1644–1659.
- [15] Masuda, S., Washizu, T., Nanba, T., *IEEE Trans. Ind. Appl.* 1989, 25, 732–737.
- [16] Chou, C., Tegenfeldt, J., Bakajin, O., Chan, S., Cox, E., Darnton, N., Duke, T., Austin, R., *Biophys. J.* 2002, 83, 2170–2179.
- [17] Cummings, E., Singh, A., *Anal. Chem.* 2003, 75, 4724–4731.
- [18] Cummings, E., Singh, A., *Microfluidic Devices and Systems III*, 4177, 2000, 164–173.
- [19] Hawkins, B., Kirby, B., *Electrophoresis* 2010, 31, 3622–3633.
- [20] Demierre, N., Braschler, T., Linderholm, P., Seger, U., van Lintel, H., Renaud, P., *Lab Chip* 2007, 7, 355–365.
- [21] Demierre, N., Braschler, T., Muller, R., Renaud, P., *Sens. Actuat. B* 2008, 132, 388–396.
- [22] Tay, F., Yu, L., Iliescu, C., *Def. Sci. J.* 2009, 59, 595–604.
- [23] Meighan, M. M., Staton, S. J. R., Hayes, M. A., *Electrophoresis* 2009, 30, 852–865.
- [24] Lapizco-Encinas, B. H., Ozuna-Chacon, S., Rito-Palomares, M., *J. Chromatogr. A* 2008, 1206, 45–51.
- [25] Clarke, R. W., White, S. S., Zhou, D., Ying, L., Klenerman, D., *Angew. Chem. Int. Ed.* 2005, 44, 3747–3750.
- [26] Clarke, R. W., Piper, J. D., Ying, L., Klenerman, D., *Phys. Rev. Lett.* 2007, 98, 198102.
- [27] Gel, M., Kimura, Y., Kurosawa, O., Oana, H., Kotera, H., Washizu, M., *Biomefluidics* 2010, 4, 022808.
- [28] Shafiee, H., Caldwell, J. L., Sano, M. B., Davalos, R. V., *Biomed. Microdev.* 2009, 11, 997–1006.
- [29] Jones, T., *J. Electrostatics* 1979, 6, 69–82.
- [30] Koneshan, S., Rasaiah, J., Lynden-Bell, R., Lee, S., *J. Phys. Chem. B* 1998, 102, 4193–4204.
- [31] Regtmeier, J., Duong, T. T., Eichhorn, R., Anselmetti, D., Ros, A., *Anal. Chem.* 2007, 79, 3925–3932.
- [32] Regtmeier, J., Eichhorn, R., Bogunovic, L., Ros, A., Anselmetti, D., *Anal. Chem.* 2010, 82, 7141–7149.
- [33] Viovy, J., *Rev. Mod. Phys.* 2000, 72, 813–872.
- [34] Smoluchowski, M., *Bull. Int. Acad. Sci. Cracov.* 1903, 8, 182–199.
- [35] Bruus, H., *Theoretical Microfluidics*, Oxford University Press, Oxford 2007.
- [36] Cummings, E., Griffiths, S., Nilson, R., Paul, P., *Anal. Chem.* 2000, 72, 2526–2532.
- [37] Jones, T., *IEEE Eng. Med. Biol.* 2003, 22, 33–42.
- [38] Shilov, V. N., *Colloid J.* 2008, 70, 515–528.
- [39] Zhou, H., Preston, M. A., Tilton, R. D., White, L. R., *J. Colloid Interface Sci.* 2005, 285, 845–856.
- [40] Simonova, T., Shilov, V., Shramko, O., *Colloid J.* 2001, 63, 108–115.
- [41] Miloh, T., *Phys. Fluids* 2009, 21, 072002.
- [42] Sung, J., Saintillan, D., *J. Fluid. Mech.* 2010, 662, 66–90.
- [43] Basuray, S., Wei, H.-H., Chang, H.-C., *Biomefluidics* 2010, 4, 022801.
- [44] Benguigui, L., Lin, I., *J. Appl. Phys.* 1982, 53, 1141–1143.
- [45] van Kampen, N., *Stochastic Processes in Physics and Chemistry*, North-Holland, Amsterdam 2007.
- [46] Jen, C.-P., Chen, T.-W., *Biomed. Microdev.* 2009, 11, 597–607.
- [47] Lapizco-Encinas, B., Simmons, B., Cummings, E., Fintschenko, Y., *Anal. Chem.* 2004, 76, 1571–1579.
- [48] Shafiee, H., Sano, M. B., Henslee, E. A., Caldwell, J. L., Davalos, R. V., *Lab Chip* 2010, 10, 438–445.
- [49] Stellwagen, N. C., *Biopolymers* 1981, 20, 399–434.
- [50] Elias, J., Eden, D., *Macromolecules* 1981, 14, 410–419.
- [51] Rau, D. C., Bloomfield, V. A., *Biopolymers* 1979, 18, 2783–2805.
- [52] Hanss, M., Bernengo, J. C., *Biopolymers* 1973, 12, 2151–2159.
- [53] Henning, A., Bier, F. F., Hölzel, R., *Biomefluidics* 2010, 4, 022803.

- [54] Bakewell, D., Ermolina, I., Morgan, H., Milner, J., Feldman, Y., *Biochim. Biophys. Acta* 2000, 1493, 151–158.
- [55] Voldman, J., Gray, M. L., Schmidt, M. A., *Annu. Rev. Biomed. Eng.* 1999, 1, 401–425.
- [56] Becker, H., Gärtner, C., *Anal. Bioanal. Chem.* 2008, 390, 89–111.
- [57] Weibel, D. B., Diluzio, W. R., Whitesides, G. M., *Nat. Rev. Microbiol.* 2007, 5, 209–218.
- [58] Kirby, B., Hasselbrink, E., *Electrophoresis* 2004, 25, 203–213.
- [59] Kirby, B., Hasselbrink, E., *Electrophoresis* 2004, 25, 187–202.
- [60] Ozuna-Chacon, S., Lapizco-Encinas, B. H., Rito-Palmares, M., Martinez-Chapa, S. O., Reyes-Betanzo, C., *Electrophoresis* 2008, 29, 3115–3122.
- [61] Martinez-Lopez, J. I., Moncada-Hernandez, H., Baylon-Cardiel, J. L., Martinez-Chapa, S. O., Rito-Palmares, M., Lapizco-Encinas, B. H., *Anal. Bioanal. Chem.* 2009, 394, 293–302.
- [62] Mela, P., van den Berg, A., Fintschenko, Y., Cummings, E. B., Simmons, B. A., Kirby, B. J., *Electrophoresis* 2005, 26, 1792–1799.
- [63] Hellmich, W., Regtmeier, J., Duong, T. T., Ros, R., Anselmetti, D., Ros, A., *Langmuir* 2005, 21, 7551–7557.
- [64] Belder, D., Ludwig, M., *Electrophoresis* 2003, 24, 3595–3606.
- [65] Makamba, H., Kim, J. H., Lim, K., Park, N., Hahn, J. H., *Electrophoresis* 2003, 24, 3607–3619.
- [66] Zhou, J., Ellis, A. V., Voelcker, N. H., *Electrophoresis* 2010, 31, 2–16.
- [67] Hellmich, W., Regtmeier, J., Duong, T. T., Anselmetti, D., Ros, A., *Langmuir* 2005, 21, 7551–7557.
- [68] Davalos, R. V., McGraw, G. J., Wallow, T. I., Morales, A. M., Krafcik, K. L., Fintschenko, Y., Cummings, E. B., Simmons, B. A., *Anal. Bioanal. Chem.* 2008, 390, 847–855.
- [69] Sabouchi, P., Huber, D. E., Kanouff, M. P., Harris, A. E., Simmons, B. A., *12th International Conference on Miniaturized Systems for Chemistry and Life Sciences (iTAS)*, 2008, San Diego, USA, 50–52.
- [70] Xuan, X., *Electrophoresis* 2008, 29, 33–43.
- [71] Erickson, D., Sinton, D., Li, D., *Lab Chip* 2003, 3, 141–149.
- [72] Baylon-Cardiel, J. L., Lapizco-Encinas, B. H., Reyes-Betanzo, C., Chavez-Santoscoy, A. V., Martinez-Chapa, S. O., *Lab Chip* 2009, 9, 2896–2901.
- [73] Kwon, J.-S., Maeng, J.-S., Chun, M.-S., Song, S., *Microfluid. Nanofluid.* 2008, 5, 23–31.
- [74] Chavez-Santoscoy, A. V., Baylon-Cardiel, J. L., Moncada-Hernandez, H., Lapizco-Encinas, B. H., *Sep. Sci. Techn.* 2010, 46, 384–394.
- [75] Thwar, P. K., Linderman, J. J., Burns, M. A., *Electrophoresis* 2007, 28, 4572–4581.
- [76] Barbulovic-Nad, I., Xuan, X., Lee, J. S. H., Li, D., *Lab Chip* 2006, 6, 274–279.
- [77] Ying, L., White, S., Bruckbauer, A., Meadows, L., Korchev, Y., Klenermann, D., *Biophys. J.* 2004, 86, 1018–1027.
- [78] Cho, Y.-K., Kim, S., Lee, K., Park, C., Lee, J.-G., Ko, C., *Electrophoresis* 2009, 30, 3153–3159.
- [79] Baylon-Cardiel, J. L., Jesus-Perez, N. M., Chavez-Santoscoy, A. V., Lapizco-Encinas, B. H., *Lab Chip* 2010, 10, 3235–3242.
- [80] Chen, D., Du, H., *Microfluid. Nanofluid.* 2010, 9, 281–291.
- [81] Zhu, J., Xuan, X., *Electrophoresis* 2009, 30, 2668–2675.
- [82] Bogunovic, L., Eichhorn, R., Reimann, P., Regtmeier, J., Anselmetti, D., *14th International Conference on Miniaturized Systems for Chemistry and Life Sciences (μ TAS)*, 2010, Groningen, The Netherlands, 1034–1036.
- [83] Kang, K. H., Kang, Y., Xuan, X., Li, D., *Electrophoresis* 2006, 27, 694–702.
- [84] Lewpiriyawong, N., Yang, C., Lam, Y. C., *Biomicrofluidics* 2008, 2, 34105.
- [85] Srivastava, S. K., Baylon-Cardiel, J. L., Lapizco-Encinas, B. H., Minerick, A. R., *J. Chromatogr. A* 2011, 1218, 1780–1789.
- [86] Hawkins, B. G., Smith, A. E., Syed, Y. A., Kirby, B. J., *Anal. Chem.* 2007, 79, 7291–7300.
- [87] Zhang, L., Tatar, F., Turmezei, P., Bastemeijer, J., Mollinger, J., Piciu, O., Bossche, A., *J. Phys.: Conf. Ser.* 2006, 34, 527–532.
- [88] Chen, K. P., Pacheco, J. R., Hayes, M. A., Staton, S. J. R., *Electrophoresis* 2009, 30, 1441–1448.
- [89] Staton, S. J. R., Chen, K. P., Taylor, T. J., Pacheco, J. R., Hayes, M. A., *Electrophoresis* 2010, 31, 3634–3641.
- [90] Zhu, J., Xuan, X., *J. Colloid. Interface Sci.* 2009, 340, 285–290.
- [91] Zhu, J., Tzeng, T.-R. J., Xuan, X., *Electrophoresis* 2010, 31, 1382–1388.
- [92] Church, C., Zhu, J., Nieto, J., Keten, G., Xuan, E. I. X., *J. Micromech. Microeng.* 2010, 20, 065011.
- [93] Ai, Y., Park, S., Zhu, J., Xuan, X., Beskok, A., Qian, S., *Langmuir* 2010, 26, 2937–2944.
- [94] Sabouchi, P., Morales, A. M., Ponce, P., Lee, L. P., Simmons, B. A., Davalos, R. V., *Biomed. Microdev.* 2008, 10, 661–670.
- [95] Jen, C.-P., Huang, C.-T., Weng, C.-H., *Microelect. Eng.* 2010, 87, 773–777.
- [96] Jen, C., Huang, C., Shih, H., *Microsyst. Technol.* 2010, 16, 1097–1104.
- [97] Lee, S.-W., Yang, S.-D., Kim, Y.-W., Kimura, Y.-K., *Conference of IEEE Engineering in Medicine and Biology Society*, 1994, Baltimore, USA, 1019–1020.
- [98] Suehiro, J., Zhou, G., Imamura, M., Hara, M., *IEEE Trans. Ind. Appl.* 2003, 39, 1514–1521.
- [99] Zhou, G., Imamura, M., Suehiro, J., Hara, M., *Proceedings of the 37th IAS Annual Meeting Industry Applications Conference*, Pittsburgh, USA, 1404–1411.
- [100] Lapizco-Encinas, B., Simmons, B., Cummings, E., Fintschenko, Y., *Electrophoresis* 2004, 25, 1695–1704.
- [101] Moncada-Hernandez, H., Lapizco-Encinas, B. H., *Anal. Bioanal. Chem.* 2010, 396, 1805–1816.

- [102] Gallo-Villanueva, R. C., Jesus-Perez, N. M., Martinez-Lopez, J. I., Pacheco, A., Lapizco-Encinas, B. H., *Microfluid. Nanofluid.* 2011, 10, 1305–1315.
- [103] Lapizco-Encinas, B. H., Davalos, R. V., Simmons, B. A., Cummings, E. B., Fintschenko, Y., *J. Microbiol. Meth.* 2005, 62, 317–326.
- [104] Chou, C., Zenhausern, F., *IEEE Eng.Med.Biol.* 2003, 22, 62–67.
- [105] Ai, Y., Qian, S., Liu, S., Joo, S. W., *Biomicrofluidics* 2010, 4, 13201.
- [106] Kang, Y., Li, D., Kalams, S. A., Eid, J. E., *Biomed. Microdev.* 2008, 10, 243–249.
- [107] Jaeger, M., Uhlig, K., Schnelle, T., Mueller, T., *J. Phys. D* 2008, 41, 175502.
- [108] Voldman, J., *Annu. Rev. Biomed. Eng.* 2006, 8, 425–454.
- [109] Barrett, L. M., Skulan, A. J., Singh, A. K., Cummings, E. B., Fiechtner, G. J., *Anal. Chem.* 2005, 77, 6798–6804.
- [110] Church, C., Zhu, J., Wang, G., Tzeng, T.-R. J., Xuan, X., *Biomicrofluidics* 2009, 3, 44109.
- [111] Gallo-Villanueva, R. C., Rodriguez-Lopez, C. E., de-la Garza, R. I. D., Reyes-Betanzo, C., Lapizco-Encinas, B. H., *Electrophoresis* 2009, 30, 4195–4205.
- [112] Prinz, C., Tegenfeldt, J. O., Austin, R. H., Cox, E. C., Sturm, J. C., *Lab Chip* 2002, 2, 207–212.
- [113] Swami, N., Chou, C.-F., Ramamurthy, V., Chaurey, V., *Lab Chip* 2009, 9, 3212–3220.
- [114] Parikesit, G. O. F., Markesteijn, A. P., Piciu, O. M., Bossche, A., Westerweel, J., Young, I. T., Garini, Y., *Biomicrofluidics* 2008, 2, 24103.
- [115] Everwand, M., Anselmetti, D., Regtmeier, J., *14th International Conference on Miniaturized Systems for Chemistry and Life Sciences (μ TAS)*, 2010, Groningen, The Netherlands, 19–21.
- [116] Kuhn, S., *Capillary Electrophoresis: Principles and Practice*, Springer, Berlin 1993.
- [117] Zorbas, H., *Bioanalytics: Methods on Molecular Biotechnology and Modern Biotechnology*, Wiley, New York 2010.
- [118] Schoch, R. B., Han, J., Renaud, P., *Rev. Mod. Phys.* 2008, 80, 839–883.
- [119] Squires, T. M., *Lab Chip* 2009, 9, 2477–2483.
- [120] Porschke, D., *J. Biophys. Chem.* 1997, 66, 241–257.
- [121] Hölzel, R., *IET Nanobiotechnol.* 2009, 3, 28–45.
- [122] Skulan, A. J., Barrett, L. M., Singh, A. K., Cummings, E. B., Fiechtner, G. J., *Anal. Chem.* 2005, 77, 6790–6797.
- [123] Hölzel, R., Calander, N., Chriagwandi, Z., Willander, M., Bier, F., *Phys. Rev. Lett.* 2005, 95, 128102.
- [124] Tuukkanen, S., Kuzyk, A., Toppari, J., Häkkinen, H., Hytönen, V., Niskanen, E., Rinkiö, M., Törma, P., *Nanotechnology* 2007, 18, 295204.
- [125] Yamanashi, S. S. T., Tazawa, S., Kurosawa, O., Washizu, M., *IEEE Trans. Ind. Appl.* 1998, 34, 75–83.
- [126] Srivastava, S. K., Gencoglu, A., Minerick, A. R., *Anal. Bioanal. Chem.* 2011, 399, 301–321.
- [127] Simmons, B. A., McGraw, G. J., Davalos, R.V., Fiechtner, G. J., Fintschenko, Y., Cummings, E. B., *MRS Bull.* 2006, 31, 120–124.